TreeD

The design, implementation and control of a 3D printer head for a composite material

Authors:
Gabriella Björk
Andreas Egneblad
Gustav Hindriks
Petter Lagusson
Johanna Nordlöf
Aron Nygren
Per von Wowern

Supervisor:
Björn Möller

December 20, 2016

KTH Royal Institute of Technology

MF2059 Mechatronics, Advanced Course

Abstract

This report addresses the use of wood materials as an alternative to plastics in 3D processing and additive manufacturing. Being able to use wood materials has many environmental advantages to using plastics, which is the material most commonly used in 3D processing today. This project was carried out by students taking the Mechatronics Advanced Course at the Royal Institute of Technology in collaboration with Innventia, a research institute working with innovations based on forest raw materials. The problems identified regarded keeping the fibers intact, as well as increasing the ratio of wood fibers from existing materials. These problems were addressed using the method continuous filament fabrication, in which a fused filament fabrication 3D printer was modified in order to operate with the added functionality. The printer head was designed to print using a paper thread consisting of spruce and pine fibers, reinforced with biodegradable PLA plastic. The stress strain tests performed showed that the composite material had the same yield strength of 27 MPa as the binding material PLA, even though the tensile specimen of the composite material weighing 17 % less. The amount of wood fibers in the composite material was calculated to around 50 %.

Acknowledgments

During this project we have gotten invaluable help without which we wouldn't have been able to finish the project. Among all the professional persons we have met during the project there are some we would like to lift.

Firstly, we would like to thank Björn Möller who has supervised and coached us through the whole project. Without your inputs and your positive attitude we would not be where we are today. Thank you for your time and all your support.

We are also grateful for all the feedback and ideas we have gotten from the rest of the teaching team in the course.

Furthermore we would also like to thank Patrik Hellgren and Tomas Östberg who has help us with construction and construction related questions and to Martin Öberg at the department of Applied Physics for help with the tensile stress tests. Also, thanks to Patrick Rohlmann for help with measuring the wood fiber ratio.

A special thanks goes to Innventia for the chance to do this project and for the feedback during the course.

Last but not least, thanks to our class in the Mechatronics Advanced Course for many laughs and ping pong-breaks between the meetings.

TreeD Group
Andreas, Aron, Gabriella, Gustav, Johanna, Per & Petter

Stockholm, December 2016

Contents

Abbreviations

AM Additive Manufacturing

CFF Continuous Filament Fabrication

DC Direct Current

FFF Fused Filament Fabrication

KTH Kungliga Tekniska Högskolan / Royal Institute of Technology

LOM Laminated Object Manufacturing

MOSFET Metal–Oxide–Semiconductor Field-Effect Transistor

PEEK Polyether Ether Ketone

PLA Polylactic Acid

PWM Pulse Width Modulation

RAMBo RepRap Arduino-Compatible Mother Board

SDL Selective Deposition Lamination

SEK Swedish Krona

SOTA State of the Art

Nomenclature

F External forces on the printer head

F_d Maximum Detent Torque

F_H Holding Torque

F_{tot} Total Friction

g Gravity acceleration constant

I Phase current in the motor

I_{CHOP} Maximum output current for stepper driver

I_{TRIP} Maximum current percentage

J_l Load Inertia

J_m Motor Inertia

J_{tot} Total Inertia

L Inductance in the coils

M Printer head mass

m_x Test mass for the simulation

μ Friction constant

ω Angular velocity of the motor shaft

ϕ Step angle in degrees

Ψ Flux Linkage

r Radius of the motor shaft (x-movement)

R Reststance in the coils

$R2$ Current sense resistor

$R3$ Current sense resistor

t Time

T_L Mechanical Torque Load

θ Angular position of the motor shaft

U Input voltage in simulation

V_{REF} Voltage Reference value

x Position of the printer head

1 Introduction

For more than twenty years there has been a continuing growth in the 3D-printing industry [1]. In recent years the research and development regarding 3D-printing materials has increased. The main interest for this project is 3D-printing techniques and materials. This project is a collaboration with Innventia, a world-leading Swedish material research institute. Their role in the project is to provide insight regarding the materials to be used in the final prototype. This section will present the background to the project, the problem formulation, delimitations and method.

1.1 Background

Today 3D printing/Additive Manufacturing (*AM*) techniques use materials such as liquid, solid and powder polymers; powder metals; and ceramics [2]. *AM* refers to creating layer-by-layer three-dimensional objects using computer-aided design [3]. The major advances from using *AM* are the time and cost reduction, as well as the possibility to create almost any shape that could be difficult to machine. The most common material of use is although synthetic polymers, more known as plastics. Conventional plastic, which is mainly used, is made from petrochemical synthetic polymers. These are extensively used in a wide range of applications, e.g. for packaging, automobile, construction etc. [4].

There are several environmental issues related to the use of plastics in our products. Plastic pollution is a huge problem in the world today. It is globally distributed across all oceans due to its properties of buoyancy and durability [5]. According to Rochman et al., synthetic polymers in the ocean should be regarded as hazardous waste [6], due to the absorption of toxicants to plastic while traveling through the environment [7]. Plastic pollution impacts and endangers marine fauna, seabirds, and marine reptiles. According to Eriksen et al., in 2014, an estimation of at least 5.25 trillion plastic particles weighing 268,940 tons was floating in the sea [8]. This is far from the only issue related to the use of plastics. As described by Amin et al. [9], "The low degradability behavior of plastics is an important environmental problem. The end-use of plastic creates waste-disposal problems as these plastics do not readily or naturally degrade and gives severe effect when plastic-waste requires more time to break down".

There is however an other alternative being presented as a high promising solution to the environmental problem of conventional non-biodegradable plastics. The solution, emerging from the bio-polymer industries advance in this field, is biodegradable plastics [9]. Biodegradation can be defined as the process in which organic substances are broken down by microorganisms such as bacteria, fungi and algae. Biodegradable plastics are derived from starch-based tubers such as sugar cane, cassava, tacca, and corn [10]. In Sweden up to this point, bio based plastics have not yet been created from the forest [11]. There is an initiative by SEKAB called Locally Produced Plastics to research whether it is possible or not to produce a biodegradable plastic from the Swedish forest. They have found that the demand for the finished product as well as the technology to create the material is already in place, but can not be implemented due to the lack of political incentives to facilitate investment decisions [11].

Sweden has a large wood industry as well as being a world-leading exporter of paper, pulp and sawn timber [12]. Being able to make *AM* using wood material would have many environmental advantages to using plastics, especially conventional plastic. Innventia is developing ideas and concepts to make wood and wood component materials of choice in 3D processing. To reach further in the innovation process a better understanding of how to produce and process wood derived based components are needed. Fundamentally it is important to better understand the flow dynamics during the filament extrusion and how wood derived entities, e.g. fibers, fiber fragments or other solid components, mix, disperse and influence process ability and filament quality. Innventia has developed a pre-mixed filament containing 70 % of the biodegradable plastic Polyactic Acids (PLA) and 30 % of wood fibers, but are experiencing problems with the wood fibers being chopped in the process, reducing the mechanical properties of the material.

1.2 Problem Formulation

The goals of this project are identified as following:

- Adapt AM using material reinforced with wood fibers
- Keep the wood fibers intact
- Increase the ratio of wood fibers from existing methods

1.3 Deliminations

This project is a masters project performed by seven mechatronics master students at the Royal Institute of Technology in Sweden. The course covers 19.5 credits, which is equal to 13 weeks of work per person. The budget was set to 50.000 SEK. The costs of the project can be found in Appendix H. Further, limitations in knowledge about the material and limited time for research had influence in choice of materials for printing etc. Since this was a mechatronics project the focus was on the mechatronics rather than the materials, and the aim was to prove the concept of the printer.

1.4 Method

The development model used in this project was based on the V-model. The problem formulation was stated as soon as Innventia had presented their ideas and after that a SOTA-research could be accomplished where interesting manufacturing methods could be researched. Functional requirements were set up early in the process from which design of the system and subsystems could be done. Definitions of the goals and problems in the project were set up. Realization and integration of the subsystems was made and verified towards the stated subsystems throughout the project with feedback loops.

All prototyping have been done at KTH and parts and materials have been ordered from KTH's chosen suppliers. Most components have been manufactured by the team, but some components were outsourced to full-time manufacturers working at the department of machine design, such as the coating mechanism described in Section 6.3.

2 Literature Study

This section describes the literature study of materials that could be used as well as the State of the Art (*SOTA*) regarding printing methods of interest, i.e. the basis for the design decisions made in the project.

2.1 Material

Understanding the characteristics and behaviors of the materials to be used in the final prototype is an important aspect of this project. The materials investigated are Cellulose-PLA Super Material originating from Innventia, PLA, natural fibers, lignin, commingled material and paper.

2.1.1 Cellulose-PLA Super Material

Innventia has investigated certain demands on materials, such as transparency for food packaging. The solution they have found is to mix *PLA* and cellulose fibers, which makes the material's characteristics depend on the heat and force with which it is pressed. [13] By doing this, only one material is needed for the packaging, instead of paper for the box and plastics for the transparent window. If the *PLA* originates from local producers, and the super material is recycled after use, this is highly environmentally friendly. Bags made of the Cellulose-*PLA* material has also been shown to be lighter than traditional paper bags in the same size.

2.1.2 PLA

As mentioned in the section above the filament material developed by Innventia contains the biodegradable plastic *PLA*. *PLA*, which is a synthetic polymer derived from natural monomers [14], is not a new polymer [15]. Interest in the manufacture of an aliphatic polyester from lactic acids was pioneered already in 1932 [16], but it was not until 1972 that high-strength, biocompatible fibers, which are copolymers of lactic and glycolic acids, were introduced. Their application was restricted until the late 1980s, when advances in the bacterial fermentation of D-glucose obtained from corn made it considerably cheaper to obtain lactic acid [15]. The *PLA* used in Innventias developed filament material is derived from corn in the USA, which is then manufactured in Japan before transported to Sweden.

2.1.3 Natural Fibers

Natural fibers have been used in various works on the applications as composite materials. For example pineapple, sisal [17], coconut coir [18], jute, palm, cotton, rice husk, and bamboo have been used in various tests where tensile strength and young modulus have been tested. [19] In this project wood fibers are of interest, and since wood itself is a composite, it has been useful to examine the methods used for the different natural fibers mentioned above. Natural fibers are gaining more interest as composite materials as they have many attractive properties, such as low weight, higher stiffness and lower cost. [17] Also, environmentally friendly composites have been a hot topic recently due to the increasing environmental awareness. [20]

The natural fibers which have been interesting for application in this project are mainly spruce, pine and birch, since these are the most common trees in the Swedish wood industry. [21]

The fibers are treated differently, depending on what tests will be done. The fibers can for example be woven, as specified by Jones [22]. This method is further discussed in Section 2.2.4. Another field of application is to make threads or ropes from natural fibers, either in form of fibers woven together or as a paper thread (as discussed in Section 2.1.6).

The applications of natural fibers are plenty, and are currently used as reinforcements in composite materials for automotive, aerospace, marine, sporting goods and electronic industries [23].

2.1.4 Lignin

All natural cellulosic fibers contain lignin [23] which is a polymer in the cell walls. The structure of lignin is very complex, and the amount differs between different plants and different kinds of woods. Some examples of the composition can be seen in Table 1.

Wood is a composite material itself, and lignin works as the matrix material along with hemicellulose to enclose the cellulose fibers. The lignin has been proven vital to protect the cellulose/hemicellulose from water and other environmental conditions. [23]

Type of bio fiber	**Source**	**Cellulose**	**Lignin**
Wood	Hardwood	43-47%	16-24%
Wood	Softwood	40-44%	25-31%

Table 1: Composition of lignin and cellulose between different types of wood [23]

Lignin has been interesting in this research since it is a component of wood. If it is a possibility to use lignin as the binding substance in the final material in this project it might be a possible solution to regain the characteristics of wood.

2.1.5 Commingled Material

Commingling is a process where two or more materials are getting physically mixed or mingled to a uniformly distributed blend. Most often the term is used when a matrix material, usually plastic, is getting reinforced with fibers. These composite materials are intended to give better material properties than the components separately. The commingled material can have different shape, texture and property depending on the basic materials, blending ratio, the commingling technique used and so on. The materials are suitable for different applications and can give a wide range of properties depending on how these are processed. Usually the commingling is made by extrusion or compounding, but there are other methods as well [24].

Innventia has developed a commingled material composing of PLA and wood fibers, where the fibers are kept intact and the fiber content is up to 40%. This composite has a paper or fluffy cotton pad like texture and is produced by wet forming preferably followed by hot molding [13] [25].

2.1.6 Paper

The making of paper is an interesting subject to research in this project since paper mainly consists of wood. It is also of interest to understand how different methods of manufacturing can alter the papers material properties. Paper can also be used for 3D printing using methods called *SDL* or *LOM* which will be discussed further in Section 2.2.5

Wood mainly consists of three components, cellulose, lignin and hemicellulose. When making the pulp for paper manufacturing lignin is often removed to allow the fibers to be separated easily. The pulp can be made from four different processes, *chemical, semi-chemical, chemi-mechanical* and *mechanical pulping*. They are in order of increasing mechanical energy used and decreasing chemicals used to separate the fibers. The more chemicals used the more lignin is removed from the pulp. Thus, mechanical pulping does not remove any of the lignin. The strength of a paper can be measured from two characteristics, the strength of the individual fibers and the strength of the bonding between the individual fibers. The strength of the individual fibers is dependent of the angle of the micro fibrils that the fibers consist of. The angle of the fibrils is different in different types of wood. Paper fibers are held together by hydrogen bonding from the hydroxyl groups in cellulose and hemicellulose. As mentioned before chemical pulping decrease the amount of lignin in the paper, this is to make it stronger because ligning interferes negatively with the hydrogen bonding between the fibers [26].

2.2 State of the Art

This section presents all to the project relevant scientific reports on *AM*. It covers extrusion, *AM* with different types of fibers, Spray Up technique, Weaving Fibers and Paper 3D-Cutting. These are all methods used in industry today.

2.2.1 Extrusion

Extrusion is a technique of interest in this project since a lot of methods in *AM* are depending on some kind of extrusion. This section is about the classic use of extruders and what can be learnt from them.

Extrusion is a process that is mostly used to create objects with a fixed cross-sectional profile. One or more materials are fed into the extruder and then the materials are pushed forward and mixed by one or two big screws. At the same time the materials are heated by the shear friction from the screws and with help from external heating. When the material is mixed, i.e. no longer solid, the screw will push it through the iron die with the desired cross-section. This is possible since "during extrusion, compressive and shear, but not tensile, forces are developed in the stock, thus allowing the material to be heavily deformed without fracturing"[28] which means that you can make very complex cross-sections without the risk of the material breaking. "The main purposes of the heaters are to melt the polymer that remains in the barrel at cold startup, to assist in forming the initial melt, and to "trim" the barrel temperatures for specific purposes such as improving feed rate." [29] which makes the shape of the screw important depending on what kind of material that are being processed.

The kind of extrusion that is interesting in this project is where plastic and wood fibers are put into the extruder and made into pellets that are used for

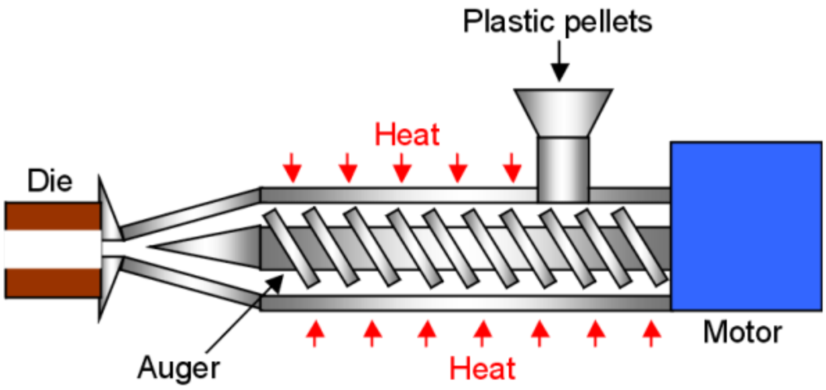

Figure 1: How extrusion works. The figure is taken from learning material from the School of Materials Science and Engineering, UNSW Australia [27]

injection molding, a process used by Innventia to try to make use of wood in new areas. The problem with putting wood fibers through an extruder is that the fibers are being crushed in the process, and the material loses the mechanical benefits gained by adding fibers.

2.2.2 3D-Printing with Fibers

There has been little research regarding 3D-printing with wood fiber materials. Therefore it is essential to also study 3D-printing with other types of fibers, such as carbon fiber, as the structure of the material is similar.

Fused Filament Fabrication FFF with fiber reinforced plastic is the most common way to 3D-print fiber materials. There is a large amount of different fiber reinforced material commercially available to use in FFF. One of these materials is e.g. WoodFill, a filament from ColorFabb, consisting of 70 % PLA and 30 % recycled fine pine wood fibers [30].

In 2000 Zhong et al. [31] showed that FFF printing with glass fiber reinforced plastic filament increased the mechanical strength of the final part compared to a non-reinforced plastic part. Furthermore Zhong et al.[31] observed that the fiberglass reduced shrinkage of the 3D-printed part. Because of the stiffness of fibers, increasing the fiber content severely effect the brittleness of the filament. A glass fiber content of more than 25 % was not possible to use with a FFF 3D printer. Filaments for FFF are manufactured using extrusion as mentioned in Section 2.2.1. Increasing the fiber content in the plastic mixture fed to the extruder results in shorter fibers in the filament produced[32].

With the aim to increase the fiber length in the 3D-printed part a new technique called Continuous Filament Fabrication CFF has been developed. It is based on a FFF machine with a few modifications. The biggest difference with FFF is that the polymer and the fiber is not bonded together before entering the print head. A few variations of the technique exists.

Matsuzaki et al.[33] have adapted a FFF printer for use with CFF. The printer head have two inlets, one for the thermoplastic filament and one for a fiber wire, in this case they use unidirectional twisted jute yarn and unidirectional carbon fiber tow. A motor driven drive gear push the filament into the nozzle. The fiber wire is fed to the nozzle inlet and impregnated with the melting plastic as shown in Figure 2. The fiber wire is pulled by the plastic filament, no extra driving mechanism is needed. It is possible to orient the direction of the fibers by adjusting the path of the nozzle. The length of the fiber is intact in the printed part. The Tensile strength of both the jute and carbon reinforced specimen was increased compared to pure PLA which was used as binding material. Furthermore Matsuzaki et al.[33] states that the carbon reinforced specimen had superior tensile strength compared to fiber reinforced plastic part made by AM. Another benefit of this method is that no pre-treatment of the fiber is necessary, which makes it possible to use a vast range of different fiber material. Matsuzaki et al. [33] assumes that it is possible to have a fiber volume of up to 50 % with this method

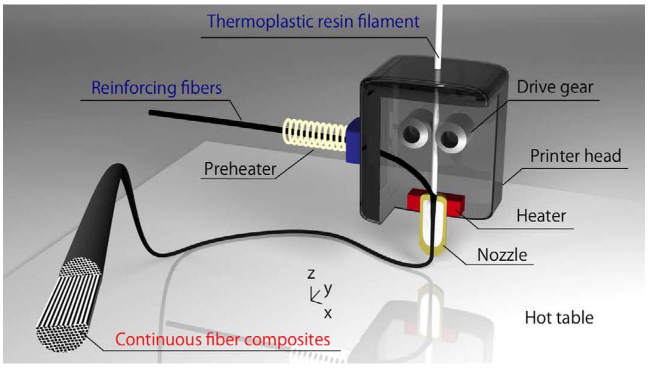

Figure 2: CFF process with one nozzle. The figure is taken from the report *"Three-dimensional printing of continuous-fiber composites by in-nozzle impregnation"* by R. Matsuzaki et al. [33]

Mark Two is a Commercial off-the-shelf 3D printer that uses CFF. It uses a nylon based polymer which is possible to reinforce with glass fiber, carbon fiber or Kevlar. The printer head has a nozzle for the nylon filament as well as a special nozzle for the fiber tow. The fiber tow is pre-coated with Nylon. The layer adhesion binds the nylon coated fiber tow with the nylon matrix on the print bed [34].

2.2.3 Spray Up

The Spray Up-process is an additive process method. A chopper gun is fed with fibers that are cut off and sprayed to a surface simultaneously with resin. The mixed material is then rolled with a roller in order to get rid of air on the surface. [35] The process is usually done manually by a operator who therefore control the thickness. The main advantage with the process is that the equipment is portable and on-site fabrication can be made.

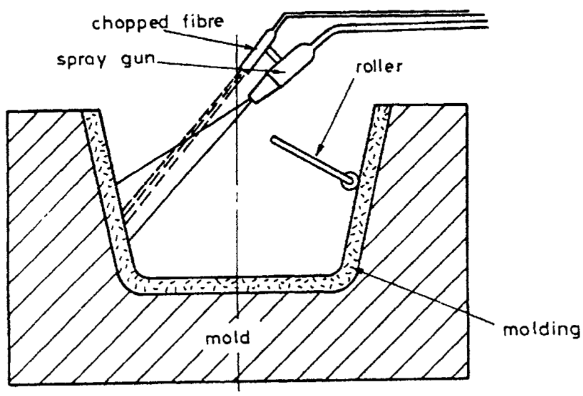

Figure 3: The spray-up process. The figure is taken from the report *"Advanced Polymer Processing Operations"* by N P Cheremisinoff [35]

2.2.4 Weaving Wood Fibers

In the method described in Section 2.2.2 the direction of the fibers are important, since Mark Two requires that the fibers are spun into a yarn like material. In cotton textiles, cotton fibers are woven into a thread, which then is used to weave a fabric. When textiles are made, the fibers has to be at least 5mm long, and according to the research in Section 2.1.3, pine and spruce have fibers which are up to 6mm long. [21] In *Mechanical Properties of Woven Banana Fiber Reinforced Epoxy Composites* [19] banana fibers are used to reinforce an epoxy material. Stress tests and Young's modulus tests are done on the material and the results showed that the characteristics of the material were good when it came to how much force it could take.

In *Mechanics of Composite Materials* [22] the characteristics of fiber-reinforced composites are discussed. When the fibers are woven perpendicularly to each other the material becomes stronger than when the fibers are woven in 45° angle.

2.2.5 Paper 3D-printing

This method consists of gluing papers together and cutting out a preferred shape using either a laser or a blade. The process is as follows. First a piece of paper is applied to the workplace, then the layer is cut according to the model from the user, glue is then applied to this layer and ultimately a new sheet of paper is applied on top and pressed against the previous layer to bond the two papers together. There are two different, yet very similar, methods to do this, *Selective deposition lamination*, *SDL* and *Laminated object manufacturing*, *LOM*. The difference between these two methods is that *LOM* applies glue uniformly to the whole layer while *SDL* deposit more glue to the area that will become the part and less to the surrounding area that is the support structure. *LOM* uses a laser while *SDL* uses a blade, usually a tungsten carbide blade, to cut the edges of the part. [36]

3 Concept Evaluation and Development

The researched methods and materials presented in Section 2 had their advantages and disadvantages. This following section covers the evaluation and development of the concept based on the SOTA in the previous section.

3.1 Concept Evaluation

This section presents the requirements developed for the prototype as well as the evaluation of printing method and materials.

3.1.1 Requirements

The aim of this project was to increase the ratio of wood fibers in *AM* without loosing the material properties and characteristics of wood. In order to achieve this a set of requirements were set up for the prototype to be developed. The requirements were divided into functional, non-functional and for material and stakeholder, and can be found in Appendix G. The decisions of concept (i.e printing method and material) was set and evaluated against a set of critical functions derived from the functional requirements. The critical functions are presented below:

- To mix wood fibers with binding substance
- To add as much wood as possible
- To control the directions of wood fibers, in x and y direction
- To keep long fibers intact
- To be able to maintain shape after print

3.1.2 Evaluation

The basis for our decision of method is by comparing each method from Section 2 with our requirement. The score is presented below in Table 2.

	Extrusion	**3D Printing**	**Spray-up**	**Weaving fibers**	**Paper 3D**
Fiber+Binder	✓	✓	✓	✓	✓
Wood Ratio	✓	✓	✓	✓	✓
Fiber Direction	x	✓	x	✓	✓
Fiber Length	x	✓	x	✓	✓
Maintain Shape	✓	✓	x	x	✓
Score	**3/5**	**5/5**	**2/5**	**4/5**	**5/5**

Table 2: Evaluation matrix for choice of concept

From Table 2 it is possible to see that 3D Printing and Paper 3D got the highest score. However, Paper 3D printing method removes material which makes it a method that consumes natural resources. Therefore 3D printing is the most preferred method.

3D-printing using FFF limited the benefits of a reinforced fiber composite. Wood fiber filaments that were available have no or very little improvement of the mechanical properties compared to the binding plastic. It was restrained both by the printing technique and manufacturing process of the filament.

However CFF adapted the FFF technique in order to use fiber composites. As described in Section 2.2.2 it could be highly customized in order to work with different fibers and binding materials. As it was possible to modify an existing FFF printer, much of the fundamental parts of the 3D printer was already done. Thus it allowed the focus on the binding and extrusion of the wood material. This led to CFF being chosen, but adapted to fit our needs. From this technique we got the possibility to choose direction of the fibers, using some sort of fiber thread, as well as maintaining their length. This meant that we could increase the amount of wood fibers (compared to $SOTA$ materials). The material needed for this is as stated earlier a fiber thread and a binding substance.

3.2 Concept Idea Development

This section presents a development of the concept from Section 3.1.2. It describes decisions that are made regarding material and machinery to use.

3.2.1 Choice of Printer

As mentioned in Section 3.1.2 a decision was made to use the CFF technique and modify a FFF printer. A decision was then made to order a 3D printer and adapt the printer head and software as it seemed feasible to achieve the requirements using this method.

A decision matrix, seen in Appendix E, was developed consisting of possible 3D printers that could be used without exceeding the project funding of 50 000 SEK, being able to be delivered within a reasonable amount of time, as well as being open source and available to modifications.

The benefits and disadvantages of the presented printers were discussed before a decision was made. Finally, the MakerGear M2 3D printer was chosen (Figure 4), mainly based on stability of the construction, i.e. the use of high quality materials and components as well as the printer head only being moved in one axis. Since the printer head prototype to be developed contains more functionality than a regular 3D-printing head the added weight could cause problems when moved on smaller axes in more than one direction. Another benefit was the open construction, making it easier to modify [37]. The 3D printer is presented in detail in Section 4.

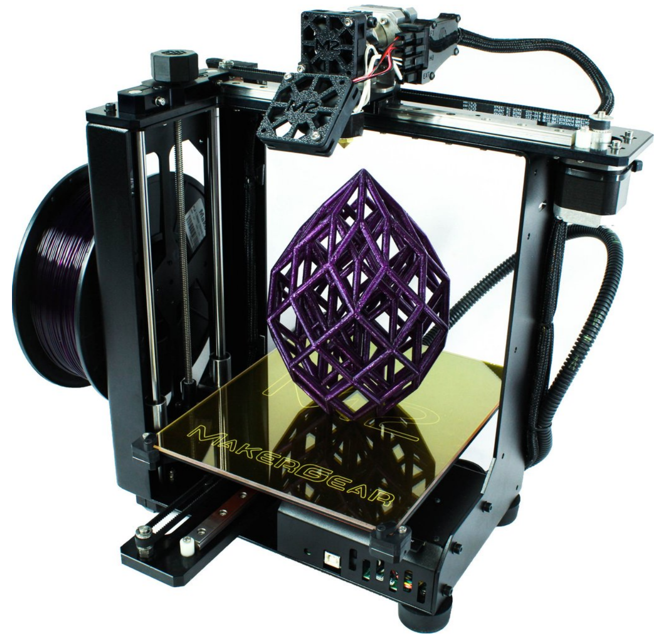

Figure 4: The Makergear M2 printer chosen for the project. This figure is taken from MakerGear's product site [37]

3.2.2 Choice of Material

For the concept chosen to proceed with, CFF, a paper thread made of wood fibers was chosen to be used as wood material. A wide variety of paper threads were ordered from distributors recommended by Innventia. There were big disparities between the different paper threads. The paper threads were evaluated regarding print-ability and strength. The following were the criteria that determined the print-ability; rigidness, bendability, size and width consistency. As all of the paper yarns bought originally was intended to be used knitting, it was hard to find a thread suited for our task. A 1 mm thick round paper thread made of kraft paper strips from the Yarn distributor Lankava was chosen. It was possible to push the thread in a given direction and it could easily be bent 90 degrees without damaging the thread. The paper thread is displayed in Figure 5.A sample of the thread was analyzed by Innventia. The analysis showed that the paper thread consist of 100 % kraft pulp made from pine and spruce. The whole report can be found in appendix A.

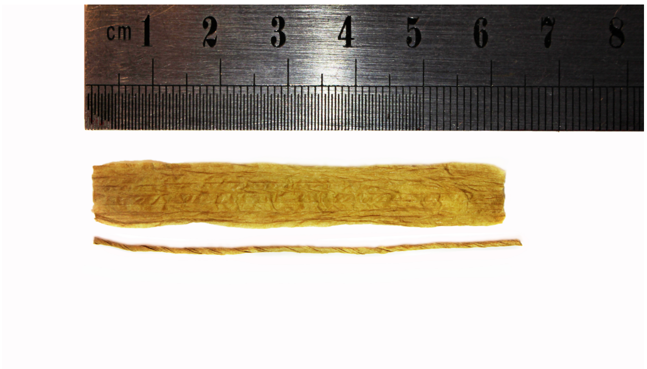

Figure 5: The paper thread, shown both twisted and untwisted. A metal ruler is used for scale

For the binding material, the use of a biodegradable plastic was an alternative with good prospects. The current *PLA* used in the filament by Innventia, due to the long transportation of both raw material and finished product, was not a sustainable solution to the problem. Unfortunately, since this project had a limited time frame and funding, using *PLA* for this prototype had to be a temporary solution.

4 MakerGear M2

This section will present the hardware and firmware of the *FFF* printer MakerGear M2 to be modified. This section only discusses the original features of the MakerGear M2 printer. Alterations and new parts are discussed in Section 6. The MakerGear M2 3D printer is open source and has a wiki with useful information about the printer [38].

4.1 Motors

MakerGear M2 uses stepper motors for movement and has one for each axis - X, Y and Z. The printer head only moves in direction of the X-axis, with movement made possible by a toothed belt which is attached to the stepper motor with a pulley. The stepper motor which moves the build plate in the Y-direction uses the same method, while motion in Z-axis is actuated with the stepper motor attached to a leadscrew. One additional stepper motor is used for feeding of the material, this one is attached to a 5.18:1 planetary gearbox. Stepper motors has a number of advantages to other motors, one is that the number of steps is equal to the number of control pulses. Also, it is precise and has good holding torque. [39]

The stepper motors all rotate with 1.8° per full step, and one revolution is 200 steps. The stepper motor driver chip on RAMBo divides each full step into 16 *micro*steps. Further, only the motor for movement in the X-direction is discussed since the printer head is remodeled to print composite material.

The standard steps/mm calculation is:

$$\frac{\text{Full steps per rotation} \cdot \text{Microsteps per full step}}{\text{Distance travelled in a full rotation}} \times \text{Gear ratio} \tag{1}$$

The stepper motor for movement in X-direction has a toothed belt pulley with GT2 profile and 18 teeth. One revolution of the pulley is 36mm. This gives us:

$$\frac{200 \cdot 16}{36} \times 1 = 88.888.. \approx 88.89 steps/mm \tag{2}$$

4.2 Temperature

The heater for the hot end is a cartridge heater rated at 40 W at 24 V. The hot end has a maximum temperature of 250 $°C$. Each heater is controlled by a MOSFET used as a switch. The input to the MOSFET is a signal from the microcontroller and the output is the voltage to the heaters.

The heated build platform is provided approximately 192 W at 24 V from a silicone heater. This combined with the moderate insulation of the silicone and air exposure and conduction to glass bed limits the maximum temperature to approximately 110-115 $°C$.

The sensors used for both the hot end and the heated build platform are thermistors, i.e. resistors that has a precise change in resistance following temperature change. Both thermistors has a resistance of 100 $k\Omega$ $\pm 1\%$.

The build platform heater has a slow response and is therefore not fully active until the set point is reached, and then fully inactive until it reaches a certain amount under that point, and then turned back on again in a repeatable process. The hot end on the other hand is controlled by a PID.

4.3 Motherboard

The mainboard of the Makergear M2 is the RepRap Arduino-compatible Mother Board *RAMBo* made by Ultimachine. Ultimachine is a company specialized in supplying hardware and electronics for 3D printers. *RAMBo* is designed to be a full featured motherboard for *FFF* 3D printers. It is improved and more versatile than its predecessor, the popular RAMPS board. *RAMBo* is open source so the design files and schematics are freely available. The Arduino compatible microcontroller Atmega2560 is used as the main computational unit and comes preloaded with the Arduino boot loader.The board can be seen in Figure 6.

RAMBo has a motor control part which feature interface for supporting up to six stepper motors. The driver used is the A4982 stepper motor driver chip from Allegro [40]. It is possible to micro step up to sixteenth of a step in order to get higher resolution of the motor. The driver also feature current chopping control. The current limit is connected with a digital potentiometer thus control of the current can be adjusted in firmware.

There is support for up to 4 thermistors for temperature sensing. Heaters and fans are each driven by a single MOSFET transistor. There is connectors for six endstops,one for each end point of the three axes. Rambo has three separate power rails; Heated bed, MOSFETs, Motors and logics. Each rail have it own fuse and can independently be supplied with a voltage in the range of 12-24 V. However in the M2 configuration, all the rails have a common voltage of 24 V supplied by the power supply. The power supply is a separate unit and converts mains to 24 V direct current DC.

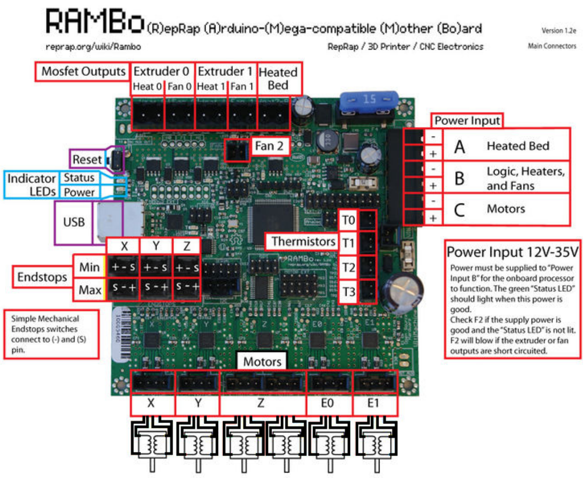

Figure 6: *RAMBo* motherboard with the most commonly used connectors highlighted [41]

4.4 Firmware

The stock firmware for Makergear M2 and *RAMBo* is Marlin. The firmware is also used among many other Arduino based *FFF* 3D printers, such as the Ultimaker 2 and the Taz 5. The main reason for using Marlin in this project is that it is an open source firmware. Marlins key functionality is to translate G-code into actions for the printer.

5 Simulation of X-axis Movement

This section will present the simulation of the X-axis movement. This was done by simulating the movement in Simulink using a stepper motor model from the Simulink library and modifying it to fit this project.

The printer head can be driven in positive and negative direction on the X-axis due to the toothed belt that is connected to the motor pulley. The simulation was done only for this motor since this is interesting considering that the alterations to the printer mainly cover the design of the printer head and its functions and therefore the mass of this part will change.

The stepper motor used to move the printer head in X-axis is a synchronous hybrid, two phased bipolar stepper motor from Kysan Electronics, serial number 42BYGH4803-C6 [42]. More information about this motor can be found in Section 4.1.

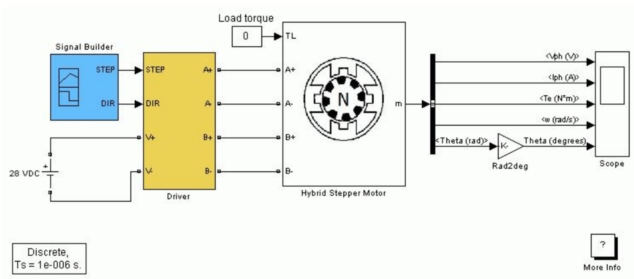

Figure 7: The model for the stepper motor from the Simulink library

The Simulink model in Figure 7 needs some data. The input voltage U was set to 24 V. The driver needs the parameters I, the phase current, and the stepping rate which is calculated as described in Section 4.1. Due to precision in the 3D printer we use microstepping to achieve the best results. $RAMBo$ divides each full step into 16 "micro"steps. The motor moves with 200 full steps per rotation and the distance traveled in a full rotation is 36 mm.

$$steps/mm = \frac{200 \cdot 16}{36} = 88.8888.... \tag{3}$$

If a desired rotational velocity ω is stated the stepping rate can be calculated. Here the rotational velocity was set to 180 mm/min.

$$\text{Stepping rate} = steps/mm \times \text{rotational velocity} \tag{4}$$

The Hybrid Stepper Motor-block takes the parameters L and R which are the winding inductance, and winding resistance. It also needs the step angle ϕ, maximum flux linkage Ψ, maximum detent torque F_d, total inertia J_{tot}, total friction F_{tot}. The initial speed and initial position were set to zero.

A simulation was done in order to decide the maximum possible weight of the printer head and to see how the mass affected the movement. The mass M was therefore varied with the masses stated in Table 3. The acronym m_x where $x = 1, 2, 3, 4, 5$, is used for the different masses.

Variable	Value [kg]
m_1	0.5
m_2	1
m_3	10
m_4	50
m_5	70

Table 3: The mass variation of the motor used in the simulation

The data sheet for the Kysan motor can be found in Appendix B. The parameters found in the data sheet are also presented in Table 4. The Maximum Flux Linkage, Ψ, produced by the magnets, the maximum Detent Torque F_d, Total Inertia J_{tot} and Total Friction F_{tot} were not stated in the data sheet. These parameters had to be calculated or estimated. The accuracy of these are discussed in Section 9.1.

According to the Simulink page the Maximum Detent Torque, F_d, can be assumed to be equal to 1-10 % of the maximum holding torque, F_H [43]. Here it was chosen to be 5 % of the holding torque.

$$F_d = 0.05 \cdot F_H \tag{5}$$

The inertia from the load, J_l was calculated as

$$J_l = M \cdot r^2 \tag{6}$$

where M is the mass of the printer head and r is the radius of the motor shaft. From this the total inertia J_{tot} was calculated as

$$J_{tot} = J_l + J_m \tag{7}$$

where J_m is the inertia of the motor. The value for J_{tot} found in Table 4 is calculated with the real measured mass of the printer head, M.

The Maximum Flux Linkage Ψ was estimated by comparing other similar Kysan motors where the value was given. The values for the total friction F_{tot} was estimated through an experiment where the printer head was detached from the motor and only was attached to the moving sleigh. The force which it needed to move was measured, and this was chosen as the estimated total friction. The friction will of course vary with the load, and is therefore seen as a heavy estimation. This is also further discussed in Section 9.1. Further, the mechanical load torque T_L was calculated as

$$T_L = r(F + \mu M g) \tag{8}$$

where r is the radius of the motor shaft, M is the mass load, g is the gravity acceleration, μ is the friction constant and F is external forces. The model is presented in Figure 8. Here F is set to zero since no further forces are considered. All parameter values can be found in Table 4.

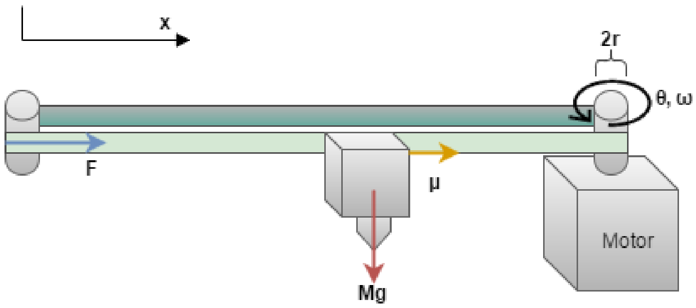

Figure 8: The load torque model

Variable	Explanation	Value	Unit	Origin
L	Winding Inductance	4.8	mH	*Datasheet*
R	Winding Resistance	2.8	Ohm	*Datasheet*
J_m	Inertia of the motor	$82 \cdot 10^{-7}$	kgm^2	*Datasheet*
ϕ	The step angle of the rotor	1.8	$Degree$	*Datasheet*
F_H	Holding Torque	5.5	$Kg \cdot cm$	*Datasheet*
I	Rated Current	1.5	A	*Datasheet*
F_d	Detent Torque	0.027	Nm	*Calculated*
Ψ	Maximum Flux Linkage	0.04	Vs	*Estimated*
J_{tot}	Total Inertia	$2.6978 \cdot 10^{-5}$	kgm^2	*Estimated*
F_{tot}	Total Friction	0.02	kgm/s	*Estimated*
r	Radius of motor shaft	0.0057	m	*Measured*
M	Mass of the printer head	0.572	kg	*Measured*

Table 4: Parameters for the motor

5.1 Simulation 1

In the first simulation the input was to drive the motor continuously in one direction with the same speed. The simulation was done for 1 s.

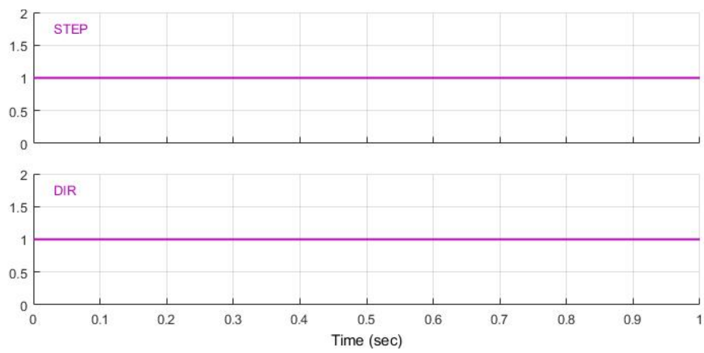

Figure 9: The input signal for simulation 1 - Driving motor in one direction

The motion of the printer head can be seen in Figure 8 where x is the position of the printer head, θ is the angular position of the rotor shaft and ω is the angular velocity. When the motor moves counter-clockwise it equals positive movement on the X-axis. $Dir = 1$ drives the motor counter-clockwise and $Dir = 0$ drives it clockwise. $Step = 1$ actuates the motor, while $Step = 0$ does not actuate. The input signal presented in Figure 9 will therefore drive the motor counter-clockwise which is positive direction on the X-axis, for 1 s.

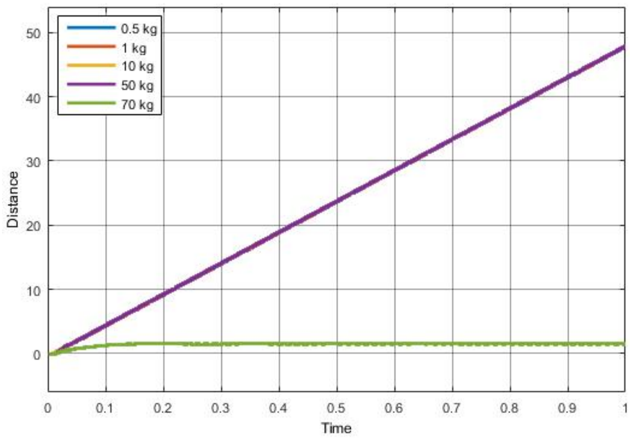

Figure 10: Output from Simulation 1

In Figure 10 it seems like mass m_1-m_4 follow a similar linear movement while m_5 does not move more than a few millimeters. In Figure 11 the graph is zoomed to compare the behavior of the different masses. The smallest masses, m_1 and m_2 move similar, while the behavior for the heavier masses, m_3-m_5 is different.

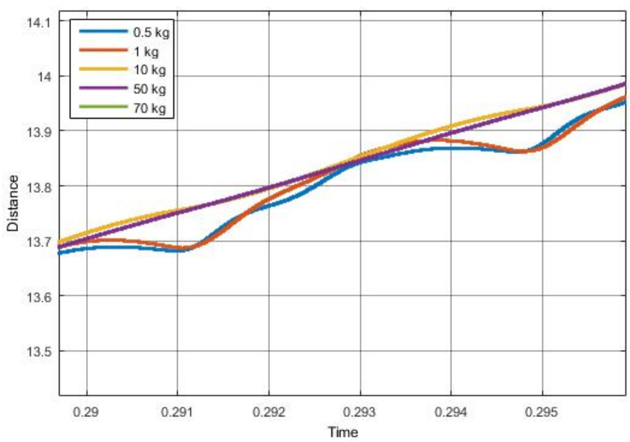

Figure 11: Zoomed view of Figure 10

5.2 Simulation 2

In simulation 2 the simulation started with keeping the printer head still, at $t = 0.1$ actuate it and move the mass in positive direction for 0.4 s. At $t = 0.5$ it should stop actuating the motor again. The movement can be seen in Figure 12.

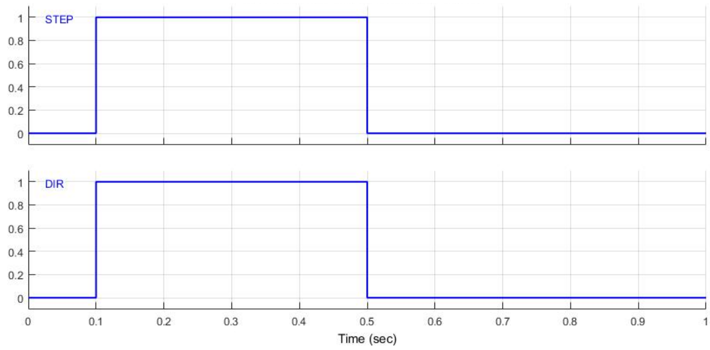

Figure 12: The input signal for simulation 2 - Driving motor with stop

The output from this simulation shows like Simulation 1 that the masses m_1-m_4 move similar, while m_5 does not move more than a few millimeter. In Figure 11 a zoomed view of 13 is shown. Here it is clear that the larger mass, the more overshoot when the printer head brakes.

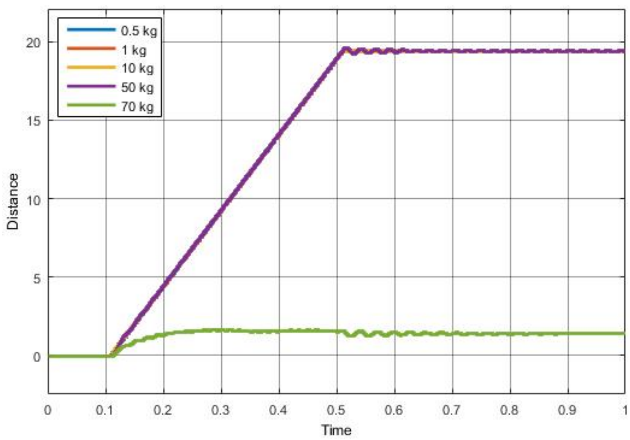

Figure 13: Output from Simulation 1

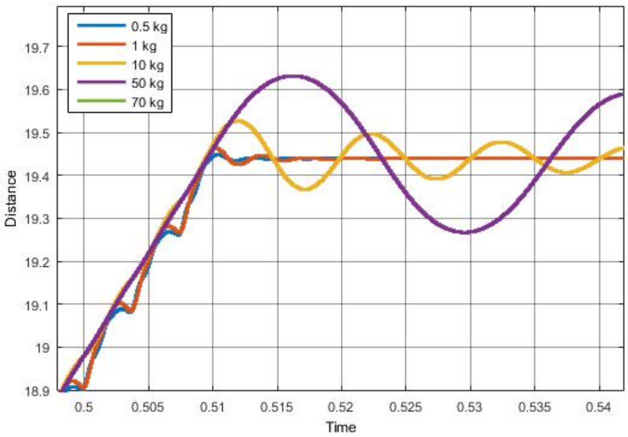

Figure 14: Zoomed view of Figure 13

6 Prototype Design

The printer head is the key part in this project. It handles both the paper thread and the plastic as well as the fusion between the two materials which is required for printing using the CFF method. As basic requirements, the printer head needs to be able to:

- Control the feeding of the paper thread
- Control the feeding of the PLA material
- Reach and maintain a temperature suitable for printing with PLA
- Coat the fiber thread with PLA so that the extruded composite filament is able to stick to the heated build platform and merge layers of filament

The coating has to be made so that the PLA is spread evenly around the paper thread and the paper thread has to be fed with enough force to pierce through the PLA and stick to the heated build platform. The materials used in the design has to be picked with great consideration of their heat transfer properties. The coating block has to be able to reach temperatures well above 200 $°C$ which makes good isolation crucial to prevent the heat from being transferred elsewhere.

This section will present the design of the printer head prototype, alterations and extra functionality added to the printer as well as the software used for printing.

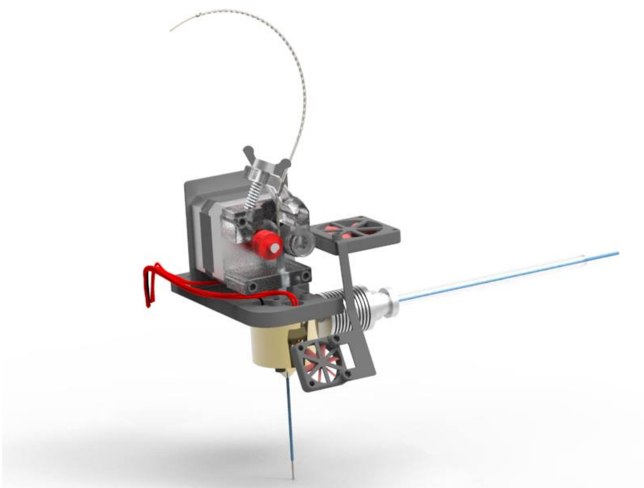

Figure 15: Final design of printer head

6.1 Feeding of the fiber thread

The thread feeding consists of two parts: pulling and pushing. The pulling of the thread, which is the first part of the feeding process, is less complex than the pushing since the pulling force is applied at the end of the thread, which will prevent the thread from bending. In theory, the thread will be pulled if the pull torque applied on the thread is larger than the counter torque from the spool inertia and the friction on the thread.

The second part of the feeding process is when the thread is pushed through the plastic and on to the heated build platform. In this process the force is applied at the beginning of the thread and has to be transferred through the thread all the way to the end. The push force at the end of the thread will be heavily reduced by any elastic behavior of the thread.

Figure 16: The thread is fed by rollers controlled by a stepper motor

In the design which can be seen in Figure 16, torque from a stepper motor is transferred to a force applied on the thread by two rollers. Since the thread used in this project is soft and has such a small diameter compared to regular plastic filament, it was decided to use two soft rollers with a high friction surface instead of the pinions which can be found in most 3D printers on the market. The thread feeder was designed with a part that can rotate around an axis to be able to tighten the rollers with a spring. The force from the spring can be adjusted by tightening and releasing a wing nut on a M3 threaded rod. This provides the capacity of feeding threads of different sizes with different levels of force requirements.

The roller on the motor shaft was 3D-printed using a flexible filament, which gave it a slightly soft surface which was taped with a fine grained sandpaper to add extra friction. The other roller consists of a ball bearing with a diameter of 16 mm and a surface with a high friction tape.

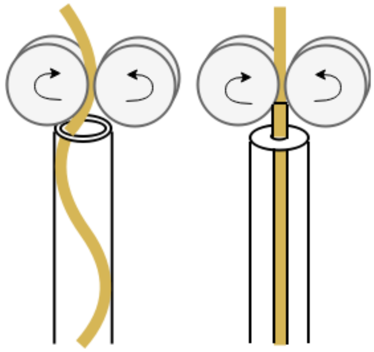

Figure 17: To the left: A too large pipe will give the thread the possibility to bend and the force from the rollers is lost. To the right: A smaller pipe inside a larger pipe prevents the thread from bending. It will also reduce the space between the rollers and the pipe.

To be able to print with a good quality, or even to print at all, the force on the thread has to be kept as constant as possible from the motor rollers where it is applied, through the coating and to the nozzle where it is pushed on to the heated build platform. To achieve this, a low friction Teflon pipe, with the same inner diameter as the thread diameter to reduce any play between thread and the pipe, is used from the motor rollers to the coating block. It is put inside a larger pipe with the same inner diameter as the outer diameter of the smaller pipe for more stability. An advantage of the smaller pipe is that i can be put closer the rollers to make sure the thread goes straight in to the pipe as seen in Figure 17.

6.2 Feeding of plastic filament

Feeding of plastic filament is one of the most common problem for FFF 3D printers. Therefore the subject of filament feeding is well investigated and there are many advanced and thoroughly designed feeders commercially available. Thus it was decided to buy an existing filament feeder rather than develop one for this project. The Bondtech QR was chosen for its robust design and previous experience with it in other projects. Conventional feeders use a motor driven knurled wheel for pushing the filament and a ball bearing for support on the other side of the filament. Two common issues with this design is slippage of the filament and friction in the bearing resulting in under extrusion. In the Bondtech extruder the ball bearing is replaced by a knurled wheel mechanically connected with spur gears to the knurled wheel attached to the motor.Thus the filament is pushed from both sides. This feature, called dual drive, results in a robust and slip free feeding mechanism. A bowden setup was used in order to avoid putting additional weight on the printer head.

A revamp of the standard calculations regarding plastic extrusion was needed considering our hot end design featured extrusion of plastic coated paper thread. The amount of plastic, i.e. the length of the plastic filament, that need to be extruded during a movement E is determined by the ratio between the cross sectional area of the plastic filament on the spool and the plastic on the coated thread. This can be seen in Figure 18.

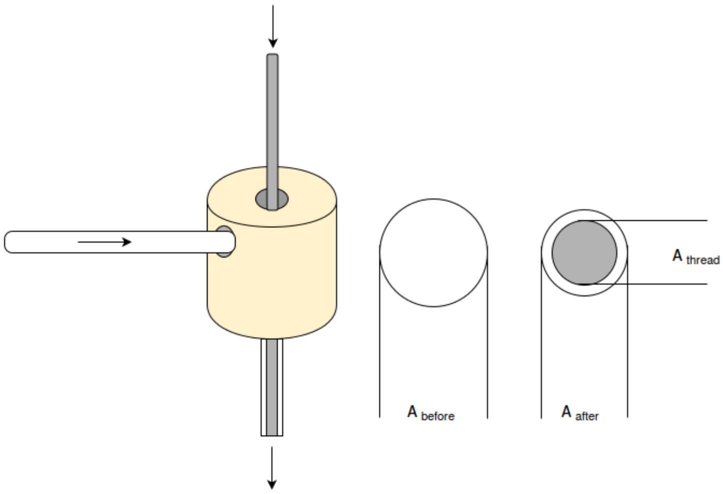

Figure 18: The white plastic enters the coating block from the left, and the fiber thread enters from the top. To be able to extrude the right amount of plastic on the thread, the plastic cross sectional area of the coated thread is compared with the original plastic filament.

Equation 9 describes how to calculate E when moving the nozzle from a point x_{start} to x_{end} with the cross sectional areas A_{before}, A_{after} and A_{thread}.

$$E = (x_{start} - x_{end}) \cdot \frac{A_{after} - A_{thread}}{A_{before}} \tag{9}$$

6.3 Coating of fiber thread with PLA

The process of printing is based on adding layers of fibers on top of each other. In order to make the layers stick to each other, coating of the thread is an essential part. The paper thread is coated with PLA to bind the printed segments together.

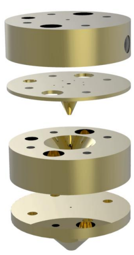

Figure 19: The coating head in exploded view

The final prototype for the coating mechanism consists of four parts, all shown in Figure 19. The parts are manufactured using milling, considering it being a relatively easy and cheap manufacturing process. The material used to manufacture the parts is brass, based on it having a good thermal conductivity, which is a key requirement in order for the mechanism to properly heat the PLA.

The PLA is fed in to the top part, seen below in Figure 20. It contains a chamber into which the PLA is melted by two cartridge heaters, further explained in Section 6.4, that are placed through all parts of the coating device to achieve an even heating of all of the parts.

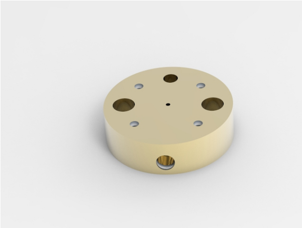


Figure 20: The top part of the coater seen from top (left) and bottom (right) view

When the chamber starts to fill up, there will be a pressure that forces the PLA to go through the middle part that has a strainer on top as seen in Figure 21. This is in order to make sure the coating of PLA is equally distributed around the thread.

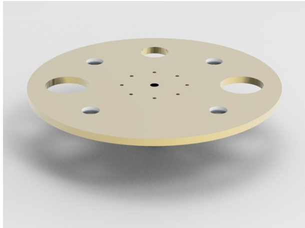
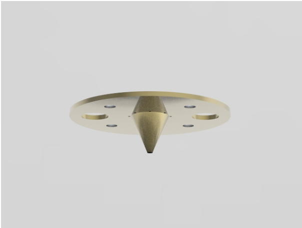

Figure 21: The strainer seen from top (left) and bottom (right) view

The bottom part is a milled container that ensures the melted PLA to go around the fiber thread, as seen in Figure 22. The diameter of the hole in the bottom part is slightly larger than the diameter of the hole in the middle part in order to make room for the paper thread to be coated with PLA. This part has threaded holes.

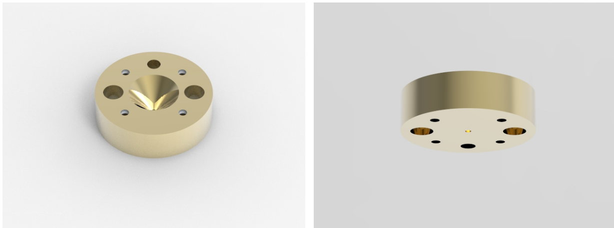

Figure 22: Middle part of coater from top (left) and bottom (right) view

The nozzle is connected to the bottom part of the coater. Originally the hole through the nozzle had a .75 mm diameter, however it was drilled to get a diameter of 1.5 mm to fit the paper thread and PLA. The edges of the nozzle opening were drilled into a cone shape with a diameter of 3 mm at the outlet and all edges were rounded to make sure the paper thread would not get stuck during extrusion. The full process of the extrusion through the coater is described in Figure 23.

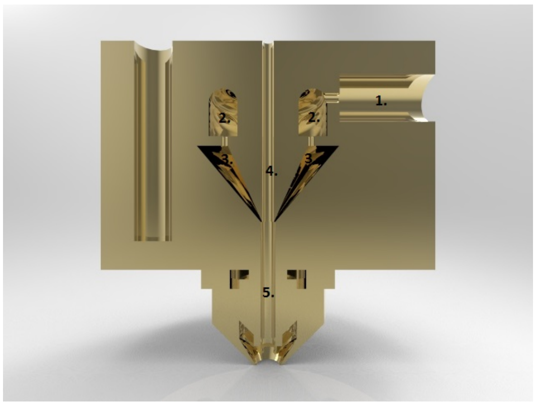

Figure 23: Section view of assembled coater

1. PLA is fed in to the coater though the heat sink
2. The PLA is melted inside the chamber by the two heating cartridges placed on the sides
3. The PLA is pushed down into the valve by the pressure from the chamber
4. The thread is fed through the coating head. The diameter of the hole is 1.2 mm
5. The PLA embraces the fiber and the coated thread is fed through the nozzle which has a diameter of 1.5 mm because the thread and plastic has larger area than the thread alone

6.4 Heat Management

In order to manage the heat transfer through the different parts of the printer head mainly five pars are used that either dissipate the heat or does not transfer it throughout the printer. The mounting plate for the coater is made of a plastic called PEEK [44], this is a material with low thermal conductivity and the reason to why this material was chosen was because it will prevent the heat from the coater to travel across the whole printer. By doing this the coater is heated much faster and energy is saved. The thermal conductivity of PEEK is 0.25 W/mK [44] which compared to aluminum, that was primarily used for this part, that has 238 W/mK. On the side of the coater there is a heat sink which will prevent the incoming plastic from melting before it is inside the coater. The fan that is mounted right above the heat sink will further increase the heat dissipation from the heat sink and keep it cold. The second fan mounted in front of the coater will help the PLA to solidify so that it sticks easier to the heated build platform and also merge the layers together. There are two 40 W heat cartridges inside the coater mounted from the top, as well as a thermistor to measure the current temperature in the coater. The thermistor used is the same one as in the original MakerGear M2 hot end explained in Section 4.2.

6.5 Electronics

This section will focus on the electronic parts of the printer head and how they are used. It will cover which stepper motor is used, which stepper driver is used and how different settings are made and also a in-house made circuit board to connect these together.

6.5.1 Stepper Motor and Driver

There were mainly two requirements on the stepper motor, firstly it should be as light weight as possible since it is mounted on the printer head and secondly it should be powerful enough to feed the paper thread without slipping. The stepper motor chosen for this project is a light weight compact bi-polar stepper motor [45]. There are mainly two components needed when driving a stepper motor, firstly a micro-controller and secondly a driver for the motor. The driver is needed because the micro-controller, Arduino Nano [46], used in this project have a current limitation that is less than the stepper motor require to work properly. This is the main reason why the driver is needed. Another benefit this driver has is that it can provide fractional steps or micro-stepping which makes the motor run more smoothly and more exact. The driver chosen in this project is the Pololu 8825 breakout board [47] that uses the DVR8825 stepper motor driver. The driver is able to provide a maximum current of 2.5 A and a maximum voltage of 45 V. This fit the requirements of the stepper motor used in this project, which has a recommended maximum current of 1.2 A and maximum voltage of 24 V [45]. Since the maximum current of the driver is higher than the rated current of the motor adjustments has to be made to reduce the maximum current going through the motor in order to not damage it. This can be done with a potentiometer provided on the breakout board of the driver.

The current through the motor windings is regulated with the H-bridges on the driver. The regulation is done by disabling the current when the current reaches a certain chopping value, I_{CHOP}, each PWM cycle. The chopping value can be set by the user using the potentiometer which regulates a voltage reference value, V_{REF}, a comparator then compares the value of V_{REF} and a current sense resistor, $R2$ and $R3$ seen in Figure 37, which are 0.1 Ω, with this equation

$$I_{CHOP} = \frac{V_{REF}}{5 \cdot R_{SENSE}} \tag{10}$$

Since the rated current for the motor is 1.2 A V_{REF} was set to 0.6 V with the potentiometer. The micro-stepping is performed with the help of an microstepper indexer which keep track of which state it is in. The state will tell the driver how much each motor winding should be energized in terms of percent of maximum current. What each state represents can be seen in table 2 in [48]. When the current hits the current percent, I_{TRIP}, in each state the windings will be placed in a decay mode which lets the current decay at different speeds that are set by the user.

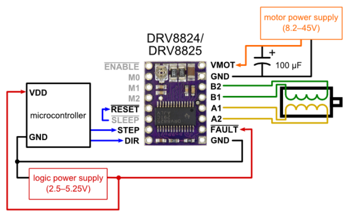

Figure 24: connection of the Pololu 8825 breakout board [47]

The stepper driver is connected to the stepper motor, power supply and the Arduino Nano as shown in figure 24.

6.5.2 Circuit board for thread feeder

A circuit board was created to minimize the amount of cables and also so that the stepper motor, stepper driver, Arduino Nano and power supply are easily connected. All these components are used for the controlling and starting of the fiber thread feeding stepper motor. The circuit board was made in DipTrace [49] and then milled. The design of the circuit board top and bottom layer can be seen in figures 35 and 36 in Appendix C. On the circuit board there is a connector for the signal that tells the stepper motor for the feeding of the paper thread to start. Two decoupling capacitors were added between the input from the motor power supply and the breakout board to reduce the risk of voltage spikes that may cause damage to the breakout board. A DC/DC converter is mounted on the board to power the Arduino Nano with 5 V. The circuit board was mounted on the right side of the 3D printer for easy access to the connectors for the stepper motor and motor power supply.

6.6 Software

The software of the system was updated in order to make it behave as desired. Since the MakerGear M2 uses open source it was possible to modify the software to its intended functions but still keep some features. In this section the G-code and print settings are presented as well as the slicer program which here was used as an interface for the printer and as a tool to monitor the self-written G-codes.

6.6.1 G-codes and print settings

Like most devices used for Computed Aided Manufacturing, the Makergear M2 3D printer operates with G-code commands. G-code are command lines which for example can tell the machine where to move in a coordinate system, set which movement speed to use and how much plastic that should be extruded during the movement. There are plenty of Software available to generate this automatically from a 3D model.

The typical commercial FFF 3D printer has the advantage of being able to print the plastic filament non continuously which means that the plastic extrusion from the nozzle can be stopped at one spot, moved to a different coordinate and restarted without having to consider the movement without extrusion. However, the 3D printer in this project uses the CFF method to print. This means that all movements in the XYZ-coordinate system has to be performed while extruding the thread. In other words: no G-code generated by a standard 3D-printing software will work. Because of this, the machine command lines that has to be written manually.

A simple example program which prints a 100 mm plastic coated fiber thread can be seen below:

```
G90 ; Set to absolute positioning
M82 ; Set extruder to absolute mode
M140 S90  ; Set bed target temperature to 90 degrees
M104 S215  ; Set extruder temperature
M109 S215  ; Wait for extruder to reach 215
M190 S90 ; wait for bed temperature to reach 90
M42 P7 S255  ; Turn on second heater
G28  ; Home all axes
G1 Y50 Z10 F9600 ; Move forward to avoid binder clips
G92 E0 ; Zero the extruder
G1 X50 Y100 F18000 ; Move to start position
G1 Z1 F181.2 ; Lower the extruder and set printing speed
M106 P0 S255 ; Start the feeding of the thread
G1 X50 Y150 E20.41 ; Move the nozzle
G91  ; Relative mode
G1 Z10 E4.081 ; Lift nozzle 10mm
M106 P0 S0  ; Stop the thread feeding
G4 ; Check if everything above is executed before continuing
M104 S0  ; Turn off extruder
G4
M42 P7 S0  ; Turn off second heater
M140 S0  ; turn off bed
G90  ; absolute mode
M84  ; disable motors
```

The code starts with telling the printer to heat up the coating block to 215 degrees using two heaters which is suitable for the PLA plastic. Since the printer only has one heater as default, the second heater is activated using the M42 command which uses a PWM signal to set the voltage over a desired output on the $RAMBo$ card. The bed temperature is set to 90 degrees. To turn on the thread feeder, a 5V signal is sent by M106 P0 S255 to the external Arduino Nano which controls the stepper motor. In order control the stepper motor a open source Arduino library was used [50]. Together with this library some additional code was added such as reading the input from the $RAMBo$ board and settings such as speed and what type of micro-stepping to be used. F is the printing speed in millimeters per minute. It needs to be the same as the speed as which the thread is fed by the stepper motor. This can be calculated using the diameter of the motor roller D_{roller} and the motor speed ω.

$$F = \omega \cdot \pi \cdot D_{roller} \tag{11}$$

The letter E in the code sets how many millimeters of plastic to extrude during the movement. This is calculated using Equation 9 in Section 6.2.

6.6.2 Slicer Program

To prepare and preview the G-code for the printer we used a slicer program called Simplify3D. In this program it is possible to preview everything the printer will do and find out if errors are made in the G-code. Simplify3D was also used to manually control the printer. It has controls for adjusting the heating and moving the printer head as well as turning the extrusion on and off. It is also possible to send single rows of G-code directly to the printer without sending a whole file which is needed since the new printer head needs a few special commands.

The slicer program was used to prepare the printer by checking that everything worked and preheating the printer head and to confirm when the printer was ready since the printer communicates with the software and sends feedback about temperatures and position back to the computer.

7 Testing

A range of tests, described in this section, were made to evaluate the printer and the printed material. The outcome of the tests can be found in the Result section.

7.1 Printing corners

Sharp turns were considered as a major challenge for the printer since a change of direction would also lead to a sudden change in direction of the force on the thread. If the thread is not stuck properly on the bed plate when turning this could lead to a misplaced thread and a decrease in accuracy. To prevent this from happening, tests were made to examine the corner behavior with different settings. The tests were carried out by drawing a reference path on the bed plate, which the printer was programmed to follow. The path can be seen in Figure 28.

Five test attempts were made. Four speed tests and one test where the printer made stops of different duration in the corners.

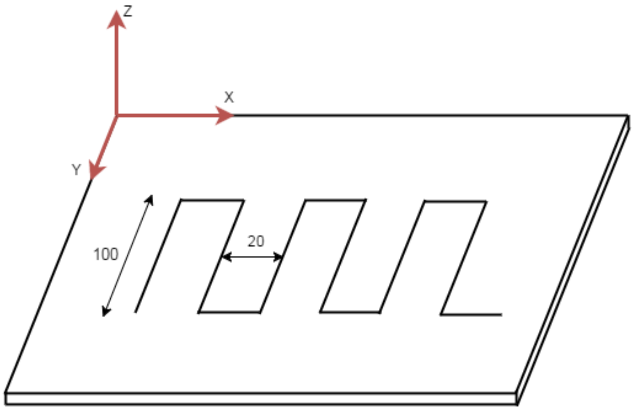

Figure 25: The test path which was used as reference in the tests. All dimensions are in millimeters.

7.1.1 Printing corners with different speeds

Four speed tests were carried out to determine how increasing the printing speed would affect the quality of the print. The different feeding speeds ω tested were 2, 4, 6 and 8 rpm. The corresponding printing speed F to each feeding speed was calculated from Equation 11 and can be seen in Table 5

ω [rpm]	F [mm/min]
2	90.6
4	181.2
6	271.8
8	362.4

Table 5: Motor speed for the thread feeder and corresponding printing speeds

A test was carried out for each printing speed where the printer followed the reference path from Figure 28 in order to evaluate how much the it would differ from the reference path.

7.1.2 Printing corners with pauses

For this test, the printer was programmed to make stops in the corners to evaluate if this would improve the quality of the print. During the stops the thread feeding, the plastic feeding and the XYZ-movement were stopped. As a reference, the path from Figure 28 was used. The test was printed from left to right and the stop time for each corner can be seen in Table 6.

Corner	Pause time [s]
1-4	0.0
5-8	1.0
9-12	2.0

Table 6: Duration of the stop for the different corners

7.2 Tensile stress test

To be able to compare the material properties of the composite material developed in this project to existing materials, tensile strain tests were made. Three different materials were compared: the TreeD composite, PLA and the WoodFill material described in Section 2.2.2.

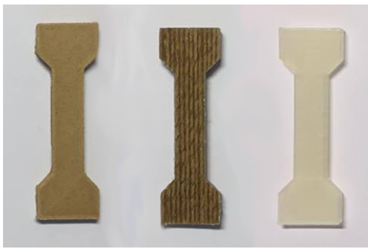

Figure 26: Tensile test specimens. From left to right: WoodFill, TreeD, PLA.

Tensile test specimens were printed for each material. However the TreeD composite specimen was printed in a rectangular shape and then cut to obtain the right dimensions. The specimens can be seen in Figure 26.

	TreeD Composite	PLA	WoodFill
Waist width [mm]	10.05	10.15	10.30
Waist thickness [mm]	3.55	3.71	3.70
Waist length [mm]	33	35	33
Total length [mm]	65	65	65
Weight [g]	3.209	3.868	3.769

Table 7: The sizes and weights of the different tensile specimens

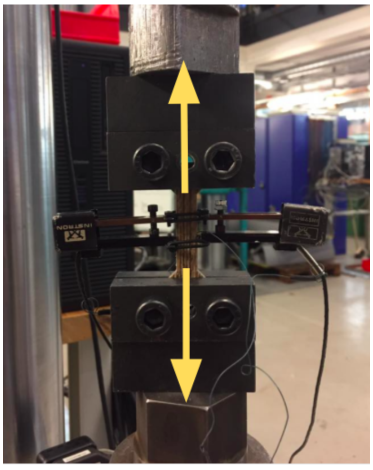

Figure 27: The setup for the tensile stress test

As Figure 27 shows, the tensile test piece is attached in both ends. Two extensiometers measure how the material extends when a force is applied. This makes it possible to obtain a strain/stress graph from which the Young's modulus for the material can be found. The test ends when the specimen breaks.

7.3 Test of fiber/PLA ratio

Both calculations and visual inspection were used in order to determine the fiber/PLA ratio of the coated thread. Assuming equation 9 is used for the extrusion of plastic, the ratio of fiber R_{fiber} of the coated thread is

$$R_{fiber} = 1 - \frac{A_{after} - A_{thread}}{A_{after}} \tag{12}$$

Where A_{thread} and A_{after}, respectively, is the area of the paper thread and the area of the thread with plastic.

For the visual inspection a Dino-Lite Premier 5 Mega pixel microscope was used. An unused tensile specimen of the TreeD Composite material was inspected. The tensile specimen was secured in a bench vice during the measurements. Only a small area of the cross section of the tensile specimen was examined, which is marked in red in Figure 28.

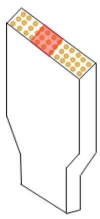

Figure 28: The end of a tensile specimen. The red area indicate the area that was used to visually determine the fiber ratio.

The Dino-Lite microscope software DinoCapture features the ability to calculate the area of drawn polygons in an image. Polygons were drawn around all the fiber threads appearing in a defined rectangular area of the cross section. Both the sum of the each area of the fiber threads and the area of the rectangle were calculated. Thus the ratio of wood fiber in the TreeD composite sample could be estimated.

8 Results

This section will present the results obtained from the tests performed, including the optimal printer settings, tensile test results and ratio of wood fibers and the assembled 3D printer.

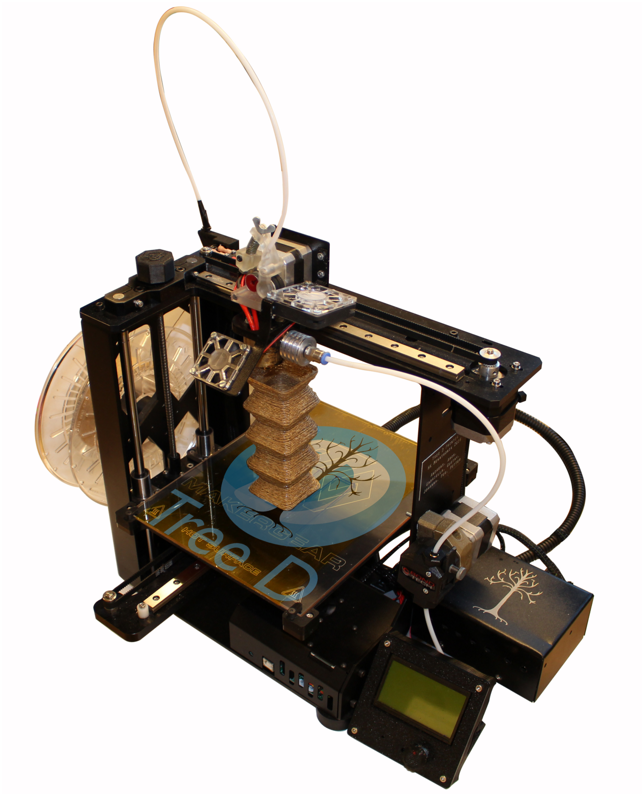

Figure 29: The assembled 3D printer.

The final design of the printer head had a mass of 0.527kg and the final design of the printer is presented in Figure 29.

8.1 Corner tests

This section will present the results obtained from the testing of different speed and stopping in corners.

8.1.1 Printing corners with different speeds

The results from the corner tests can be seen in Figure 30 and in Figure 31. The performance is evaluated by comparing the distance from the reference path (Figure 28), which is represented as the drawn black line, to the printed path.

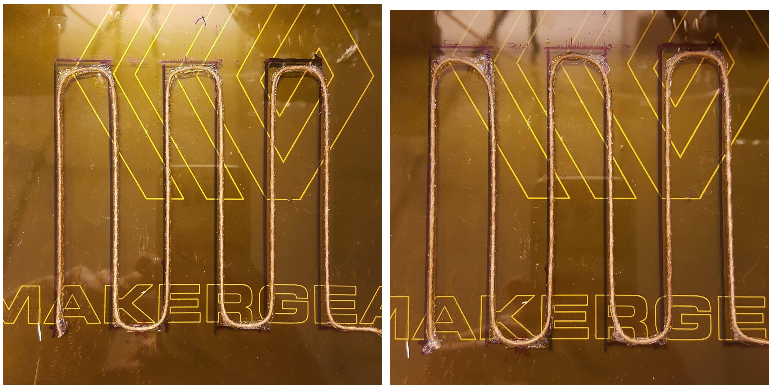

Figure 30: To the left: the thread is fed 90.6 mm/min. To the right: the thread is fed 181.2 mm/min.

As can be seen in Figure 30, the radius of the corners increases as the printing speed increases from 90.6 mm/min to 181.2 mm/min. However, the difference is not very big and not proportional to the duplication in speed.

Figure 31: To the left: the thread is fed at 271.8 mm/min. To the right: the thread is fed at 362.4 mm/min

When increasing the speed to 271.8 mm/min, as can be seen in 31 the radius of the corners increases significantly compared to what can be seen at lower speeds. The fiber thread does not have time to stick to the heated bed which decreases the sharpness of the corners. This is even more obvious when printing at 362.4 mm/min.

8.1.2 Printing corners with pauses

As in the speed test, a printed path with sharp corners as similar to the reference path as possible, was desired.

Figure 32: Pause test where corner 1-4 (from left to right) is printed without pausing, corner 5-8 is printed using pauses of 1 second in each corner, and corner 9-12 is printed with pauses of 2 seconds in each corner.

Figure 32 shows how pausing the print in the corners, has a positive effect on the quality of the print. When looking from left to right, the pause time increases every fourth corner which reduces the radius.

8.2 Tensile stress test

The stress strain curves for the materials can be seen in Figure 33. The data obtained from the tests are presented in Table 8.

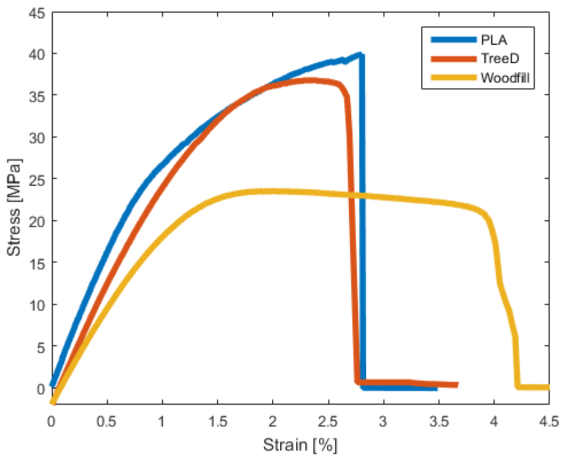

Figure 33: Stress strain curves for the three materials tested

The TreeD Composite and the binding PLA had the same yield strength of 27 MPa, although the PLA having a slightly higher ultimate tensile strength of 40 MPa compared to the composites 37 MPa. The WoodFill material, as seen in the stress strain curve, had a lower yield and ultimate tensile strength of 19 MPa respectively 24 MPa,

	TreeD Composite	PLA	WoodFill
Yield strength [MPa]	27	27	19
Ultimate tensile strength [MPa]	37	40	24
Young's modulus [GPa]	2.97	3.27	2.32

Table 8: The tested settings for the printer

8.3 Ratio of wood fiber in the composite material

According to Equation 12 the fiber ratio in the TreeD material is 44.4 %. However the visual measurements showed a 50 % content of wood fibers. Figure 34 shows the image of the cross section used in the visual inspection of the fiber ratio.

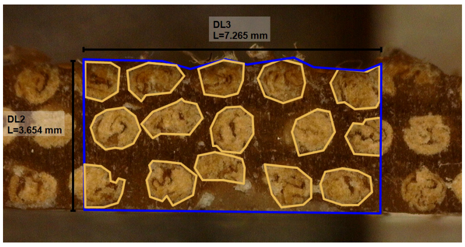

Figure 34: Visual measurement of the fiber ratio.The blue line indicates the measured area and the yellow polygons marks the boundary of the fiber threads.

9 Discussion and Conclusions

This section discusses the obtained results and also which conclusions that can be drawn from these. The discussion will mainly cover the the ratio of wood fibers in the composite material, which factors that limit the printing speed and the simulation of the printer head.

9.1 Discussion

As stated in the results the composite has a ratio of 44.4 % wood fibers. This is an result of the design of the coater and the speed of the printer and paper thread. The coater has an opening with the size of 1.5 mm whereas the paper thread is about 1 mm. To further increase the ratio of wood fibers a redesign of the coater has to be made with a smaller opening. However, since the plastic is the binding material in the composite, this may result in that the coated paper thread then will have problems sticking to the build plate and also merging the layers together as a result of the smaller amount of plastic. This has yet to be tested because of the time taken to create a new coater is too much for the limited project time.

The visual measurements showed another result than the theoretical approximation of the ratio of wood fibers in the composite. There are several reasons to why this is, firstly it is dependent of where in the sample this is calculated and secondly, it is dependent on which sample is used since they may vary from print to print. Speculations concluded that the ratio does not vary more than around than ± 10 %. This shows that the theoretical approximation is satisfactory.

The resolution of the 3D printed part is dependent on the thickness of the paper thread but also the amount of plastic in between the layers. In order to achieve a higher resolution but still keep the same ratio of wood fibers a thinner thread has to be used but also a redesign of the coater with a smaller opening so that the ratio of plastic and wood fibers are kept the same.

The speed of the printer is 180 mm/min and compared to "regular" 3D printers, which prints at a speed of around 1200 mm/min, it is quite slow. The reason to why the 3D printer is that slow is because of several reasons, firstly the plastic has to go through several steps in the coater, such as pressurize the chamber on top of the coater, get through the strain and ultimately through the cone. This process can not be to fast due to the viscosity of the melted plastic which make the plastic go through these steps quite slowly. Another reason is that it take some time for the coated paper thread to stick to the building plate as it has to solidify to some extent before it gets a good grip on the building plate and also the merging of the layers. This is clearly visible in Figures 30 to 32 where a higher speed results in that the corners do not stick to the build plate and are dragged along. When the printer head is stopped in each corner this even further increase the sticking and gives a much better result as seen in Figure 32.

The simulation in Section 5 gives an approximative value of the possible maximum weight of the printer head. However, some parameters are heavily estimated and therefore the result needs discussion. Stepper motors are known for their precision and good holding torque and compared to other motors they do not need any controlling. However, the simulation shows clearly that with increasing mass we loose some of the good precision and there is an evident overshoot when the printer head beaks from constant speed.

To improve the simulation more accurate parameters would be needed. The friction is measured experimentally and can be considered a good estimation for small masses, but since it is set constant to all experimental masses in the simulation it would need further work.

The maximum flux linkage Ψ is estimated from other Kysan Stepper motors and should also be better estimated.

In all, the simulation gives us the result that the printer head can weigh up to 70 kg, a mass that we will not even be close to. The real mass of the finished printer head was 0.527kg. Therefore it can also be discussed if the simulation was necessary at all, and if there was something more interesting to investigate in the Simulink model.

9.2 Conclusions

The prototype developed proves that the concept of printing with a composite material consisting of a fiber thread and binding material is possible as seen in Figure 38 in Appendix F.

The result of the tensile testing determined that the yield strength threshold was the same for our own composite and the PLA. The reasons to why they are equally strong even though the composite is lighter can be because it has the fibers in the same direction as the pulling force even though the binding between the layers may be weaker. With this result we can conclude that our composite is indeed stronger in terms of MPa/kg. This also proves that this concept of a 3D printer using natural materials is able to print without making the material properties in terms of strength worse, in fact it is better than just PLA in a sense.

One of the requirements, seen in Section 3.1.1, was to increase the ratio of wood fibers, this is clearly proven to be successful as the composite material has 44.4 % wood fibers and this is also a huge improvement to existing composites that have been 3D printed on the market today. As a comparison, the printed composite material presented in reference [33] only has a ratio of 6.1 % wood fibers. The requirement to be able to print in the x and y direction was also fulfilled and as an addition the printer is also able to print the in z direction.

Most of the requirements were fulfilled with exception to a few. The printer is not able to print a tensile specimen by itself due to the sharp edges it requires and the resolution for the printed object are near the requirement of 1 mm but they vary since the printer is imprecise.

To conclude the printer fulfills its most important features since it is able to print 3D object with a high ratio of natural fibers which was the main goal of the project.

10 Recommendations and Future Work

The printer head prototype developed in this project is to this point only a proof of concept. This section presents recommendations and future work that is encouraged to proceed with in order to take 3D printing of wood fibers further into the innovation process and eventually even using it industrially.

10.1 Material

The paper thread used for this prototype is one of the main limiting factors for making this a viable concept ready to use in industry. Innventia is developing wood based threads which in the future might be more well suited for this type of product. Using a more suitable thread could increase the print result tremendously.

To fully be able to create an environmentally beneficial end product using 3D printing the binding substance in the material could with further research be derived from local raw materials, such as bio based plastics from wood, instead.

10.2 Prototype

The main problem with the implemented prototype is that it can only print continuously, which limits the possibility of more complex shapes to be printed. Implementing of a cutting mechanism would make the printer a lot more versatile, and this was initially something that was considered for the prototype but had to be deprioritized as there simply was not enough time to implement it in the final design. The developed prototype for the cutting mechanism can be seen in Appendix I.

In order to make the printer more energy efficient, a reduction of heated material in the coating mechanism would be preferable, since reducing energy consumption and creating a more environmental solution is one of the main reasons for using wood in 3D printing.

There was some problems with the parts printed not maintaining their intended shape. In order to receive a better print result as well as allowing a higher print speed more fans could be implemented in the prototype, this for making sure the material cools down quicker, hence remaining the shape.

During this project a slicer program was used in order to generate initial G-code as well as illustrating the 3D shapes created by the G-code. The G-code had to be manually modified because of the continuous printing, the speeds for extrusion of plastic and paper thread not being according to standard as well as the various settings that was tested to create the best possible print. Preferably all of this would be handled automatically by the slicing program or an equivalent program, i.e. with the aim of the program being able to directly translate CAD-models into operational G-code, since writing G-code is a rather time consuming activity and human errors could affect the result. To receive an optimal print result there would also be a need to dynamically change the speed during run time depending on situation, i.e. increasing the speed when moving straight and decreasing through corners. This could also be handled by the program creating the G-code. Therefore a recommendation for creating such a solution is highly encouraged.

Appendices

A Results of analysis of paper thread

INNVENTIA

REPORT

Commission: 2016-0533
Arrived: 2016-11-08
Your order no.:
No of samples: 1

Innventia AB
Biorefining & Biobased Material
Material Design

Your ref: Mikael Lindström

Analysis of chemical composition of rope made of paper

Type of sample

The sample is a rope made of paper. Two pieces of ropes were enclosed (one about 1 mm in diameter and one about 0.5 mm in diameter. Both samples are treated as one type of paper.

Methods

The characterization of the organic content was performed using pyrolysis-gas chromatography/mass spectrometry (Py-GC/MS). The result is obtained as a so-called pyrogram, with the intensity of the pyrolysis products (total ion current, TIC) set against the retention time. Mass spectra are recorded, which enables an identification of structural types of the products. Polar compounds, especially acids and alcohols are derivatized by methylation of the sample using tetramethyl-ammonium hydroxide (TMAH).

Fibers were observed using a Zeiss light microscope Axioplan.

Electron scanning microscopy (SEM) was carried out using a Hitachi SU3500.

Objective and background

What is the paper rope made of? Type of wood? Additives? Paper thickness?

Stockholm, 05 December 2016
Innventia AB/ Chemical Analysis

Anders Reimann
Research Engineer

Phone: +46 8 6767 445
Fax: +46 8 10 83 40
E-mail: anders.reimann@innventia.com

Conclusion

- The paper rope consists of 100 % unbleached softwood (pine and spruce) Kraft pulp.
- The additive paraffin (wax) was found in the rope. Paraffin is commonly used to improve water resistance of papers. No other additive could be identified in relevant amount in the rope.
- The thicker rope has a diameter of about 1 mm, whereas the thinner rope has a diameter of about 350 µm. The paper thickness is about 40 µm.

Results

Light microscopy

The light microscopy investigation showed that the rope consists of 100 % unbleached softwood (pine and spruce) Kraft pulp. Some traces (< 1 %) of bleached hardwood Kraft pulp was also found in the sample.

Electron microscopy

In *figure 1*, electron micrographs of the paper ropes are shown. The picture to the left shows the thickness of the ropes. The thicker rope has a diameter of about 1 mm, whereas the thinner rope has a diameter of about 350 µm. The picture to the right shows a cross-section of the paper (from thicker rope). The thickness of the paper is about 40 µm.

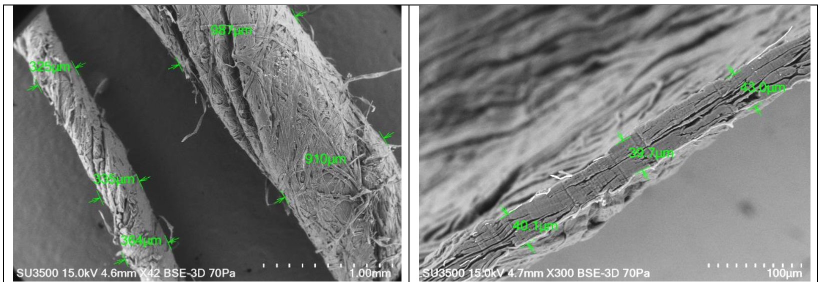

(a) (b)

Figure 1: Scanning Electron Micrographs of the two paper ropes beside each other (a). Scanning Electron Micrographs of Cross-Sections of paper (b).

Organic analysis by pyrolysis

The paper rope was analysed by analytical pyrolysis. The sample was analysed directly as it is, but also acetone extract of the rope was analysed. The analyses were performed with methylation (TMAH) for identification of both polar and non-polar compounds. In *figure 2*, pyrograms of the sample and acetone extract are shown. The pyrograms show the organic composition and illustrate the relative amounts.

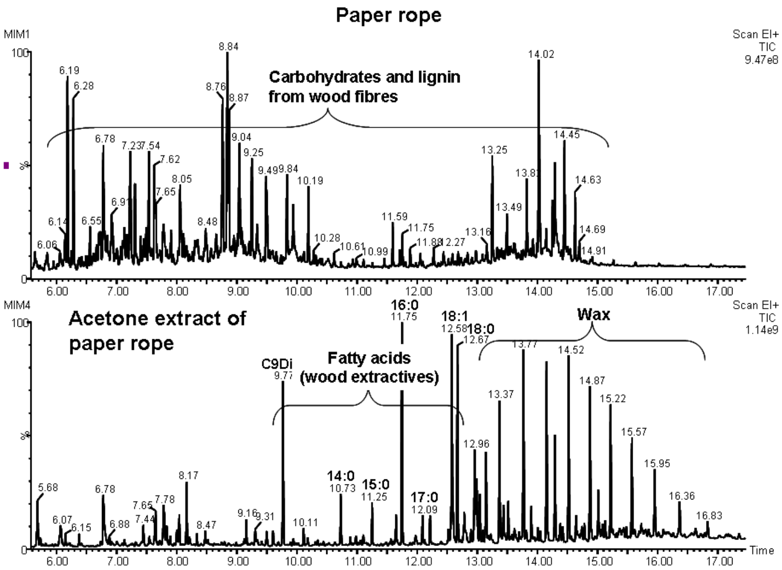

Figure 1: Pyrograms of the paper rope and acetone extract. The pyrograms show the presence of the organic components in the rope.

The upper pyrogram in *figure 2* shows the organic composition of the rope when pyrolysed directly as it is (without pre-treatment). All major compounds identified are related to carbohydrates and lignin from the wood fibres. No additives could be identified in the sample.

In order to detect additives in low amount, the rope was extracted by acidified acetone. The obtained extract were then partly evaporated and analysed by pyrolysis. The obtained results are shown in the lower pyrogram. As can be seen from the figure, the extract contains various fatty acids and wax (paraffin). All fatty acids probably derive from wood extractives. Paraffin (wax) is commonly used to improve water resistance of papers. No other additive than wax could be identified in relevant amount in the paper rope.

B Datasheet Kysan Motor

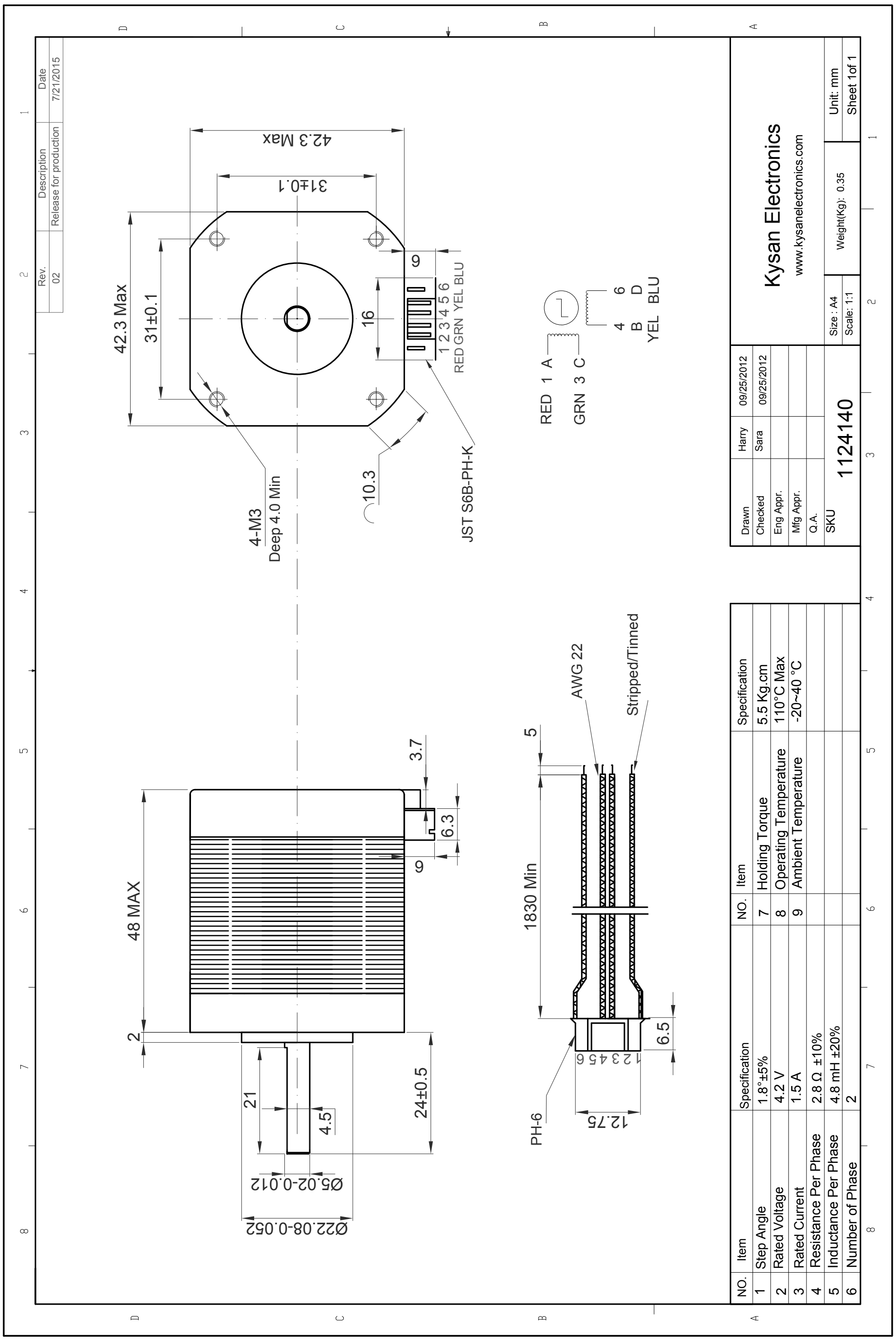

C Circuit board Design

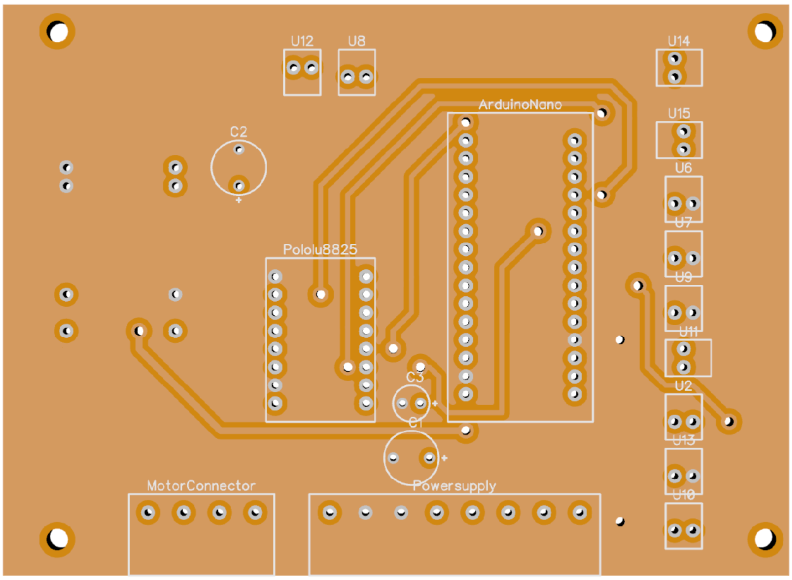

Figure 35: Circuit board design top layer

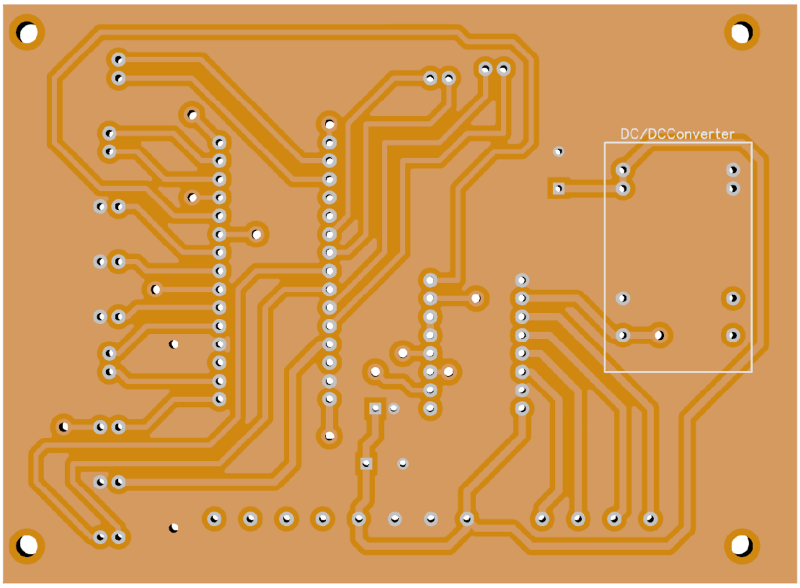

Figure 36: Circuit board design bottom layer

D Pololu 8825 breakout board

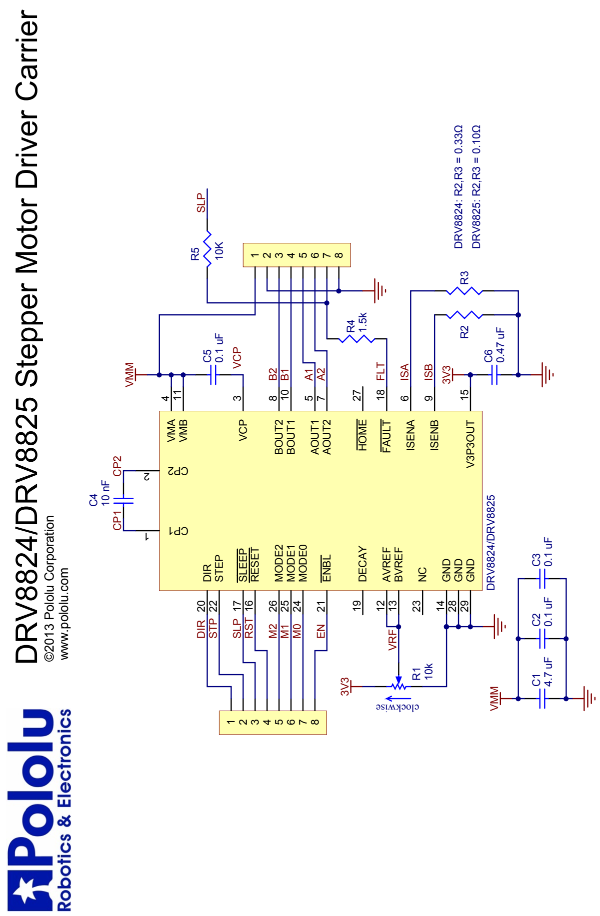

Figure 37: Schematic of the Pololu 8825 breakout board [51]

E Decision Matrix 3D Printer

Printer	Original Prusa i3 MK2 3D	LULZBOT MINI	LULZBOT TAZ 6
Company	Prusa Research s.r.o	Aleph Objects	Aleph Objects
Info about printer:			
Open Source	Yes	Yes	Yes
Build Volume (mm)	250 x 210 x 200	152 x 152 x 158	280 x 280 x 250
Movement	Head: x, z Bed: y	Head: x, z Bed: y	Head: x, z Bed: y
Top Print Speed	Not specified	275 mm/s	200 mm/s
Max. Tool Head Temperature	300 °C	300 °C	300 °C
Max. Heated Bed Temperature	Not specified	120 °C	120 °C
Self Leveling	Yes	Yes	Yes
Dual Extruder Compatible	No	No	Yes
Construction	Open construction	Open construction	Open construction
Assembled	Both assembled and DIY	Yes	Yes
Cost/Delivery info:			
Cost	DIY € 739, Assembled € 999	$ 1,250	$ 2,500
Delivery	DIY quick delivery, Assebled 3 weeks	Quick delivery. Amazon	Quick delivery. Amazon
Summary			
Pros	Low price, advanced calibrating of printer bed, Quality components, Good firmware	Low price.	Has good ratings from "Tom's Guide"
Cons	Might be a bit weak if head is heavy	Seems to be more of a "hobby" printer	Might be a bit weak if head is heavy

Velleman K8200	MakerGear M2	Magicfirm - ZYYX+	Ultimaker Original+
Velleman	MakerGear	Magicfirm	Ultimaker
Yes	Yes	Yes	Yes
200 x 200 x 200	254 x 203 x 203	265 x 225 x 195	210 x 210 x 205
Head: z, Bed: x,y	Head: x Bed: z, y	Head, x, y Bed: z	Head: x, y Bed: z
200 mm/s	400 mm/s	200 mm/s	300 mm/s
Not specified	300 °C	265 °C	260 °C
No heated bed plate	110 °C	Not specified	100 °C
No	Yes	Yes	No
No	Yes	No	No
Open construction	Open construction	Closed construction	Closed construction
DIY kit	Yes	Yes	DIY kit
4 500 SEK	$ 1,825	14 232 SEK	11 700 SEK
Quick delivery. ELFA.	Quick delivery. MakerGear.	Quick delivery. Creative Tools.	Quick delivery.
Low price. Only one axis movement of head. Easy to modify and buy spare parts	Robust construction. Only one axis movement of head.	Low price. Robust design.	Low price.
Low quality components.	Only american supplier.	Closed construction.	Closed construction.

F Printed Parts

Figure 38: Picture of printed parts

G Requirements

TreeD – Mechatronics Advanced Course
Royal Institute of Technology
2016-09-29

Requirements

Functional requirements

- The product should use additive manufacturing creating a 3D object
- The product shall produce an object using wood fibers
- The product shall be able to place the fibers in the XY-plane
- The direction of the fibers should be the same as the direction of the moving printer head
- The manufactured object of standard dimensions shall have (+/- 10%) of the tensile stress[1] as a piece of the matrix material used in the composite material
- The manufactured object standard dimensions shall have (+/- 10%) of the yield strength[2] as a piece of the matrix material used in the composite material
- The product shall be able to manufacture a tensile specimen with standard dimensions
- The machine should get the data from the computer or from a SD-card

Non-functional requirements

↑ - preferably higher
↓ - preferably lower
• - sharp value

Prio 1 = high
Prio 2 = middle
Prio 3 = low

Requirement for printer	**Value**		**Prio**
Extrusion speed of printer	100 mm/min	↑	Prio 2
Print head travel speed		↑	Prio 2
The resolution of the printed object	1 mm	↓	Prio 2
The temperature of the extruder	200˚C [3]	↑	Prio 1
The temperature of the building plate	100˚C	•	Prio 1
Ambient temperature	15 ˚C to 32 ˚C	•	Prio 2
Build dimensions	200 mm x 250 mm x 200 mm	•	Prio 3
Machine weight	Max 12kg	↓	Prio 3
Power requirements	24V	↓	Prio 2

[1] Tensile stress = brottgräns
[2] Yield strength = sträckgräns
[3] Melting temperature of PLA is 180˚C but is preferably around 200˚C during 3D-printing. The cellulose fibers can handle a temperature up to 200˚C.

Material requirements

The ratio of Swedish wood in the printing material	90%	↑	Prio 1
The ratio of wood fibers in the printed object	40%	↑	Prio 1
Amount of waste during manufacturing	5%	↓	Prio 1

Stakeholder Requirements

- The product shall not exceed 50 000 kr to manufacture

Test case

- Tensile stress test – print a tensile specimen with standard dimensions and test it to other materials

H Project costs

Cost of parts			
Part	**Quantity**	**Company**	**Price**
LayFilaments Laywood-Flex - 2.85mm - 0,25 kg	1	3d-Prima	249,00 kr
LayWoo-d3 Filament - 3mm - 0,25kg	1	3d-Prima	219,00 kr
bioFila linen Filament - 2.85mm - 750g spool	1	3d-Prima	499,00 kr
SPÅRKULLAGER S688 ZZ RFR	2	kullager.se	76,00 kr
OLJEBRONSB. FLÄNS 4/8x6-10	6	kullager.se	96,00 kr
LÅSRING SGA 4	10	kullager.se	20,00 kr
Simplify3D	1	Creative tools	1 615,00 kr
Knife Blades	1	Clas Ohlson	60,00 kr
Bondtech QR 1.75 Universal	1	Bondtech	1 604,00 kr
Adapter direct - Bowden 1.75	1	Bondtech	81,00 kr
Kiselfett 10 gram i spruta	1	Electrokit	39,00 kr
Självhäftande värmefolie 3M 8810 80x80mm	1	Electrokit	59,00 kr
Rundrem ø3.175mm 76mm	8	Electrokit	72,00 kr
PTFE slang natur Øi 1,07 x 0,30 mm AWG 18 T	2m	Nordbergstekniska	83,00 kr
PTFE slang natur Øi 1,19 x 0,30 mm AWG 17 T	2m	Nordbergstekniska	90,00 kr
PTFE slang natur Øi 1,35 x 0,30 mm AWG 16 T	2m	Nordbergstekniska	90,00 kr
PTFE slang natur Øi 0,56 x 0,25 mm AWG 24 T	2m	Nordbergstekniska	45,00 kr
PEEK platta natur tjl 6 mm remsa: 500 x105 mm	500 x105 mm	Nordbergstekniska	858,00 kr
DRV8825 Stegmotordrivare	1	3d-grottan	94,00 kr
Värmetåligt isolerande pappersark A4x1mm	4	3d-grottan	125,00 kr
Värmepatron 24V - 40W - 6x20mm	2	3d-grottan	113,00 kr
E3D Thermistor Replacement kit	1	3d-grottan	90,00 kr
Thermistor 100k with Cable	1	3d-grottan	75,00 kr
Värmetåligt isolerande pappersark A4x1mm	1	3d-grottan	32,00 kr
Värmepatron 24V - 40W - 6x20mm	2	3d-grottan	113,00 kr
Pneumatisk koppling 4mm M6	2	3d-grottan	38,00 kr
Teflonslang 2x4mm 1dm+	20	3d-grottan	119,00 kr
M6*26 Teflon printer värmebarriär 1.75mm plasttråd	1	3d-grottan	57,00 kr
E3D v6 HeatSink - 1.75mm Universal (With Bowden	1	3d-grottan	218,00 kr
Printer Nozzle Throat V6 1.75mm filament	2	3d-grottan	50,00 kr
Axiell Fläkt 25x25x10mm 24V	1	3d-grottan	38,00 kr
M6*26 printer värmebarriär 1.75mm plasttråd	1	3d-grottan	38,00 kr
Stiftlist Raster 5mm 8P	2	Elfa Distralec	12,00 kr
Honkontakt Raster 5mm 8P	2	Elfa Distralec	21,00 kr
Honkontakt Raster 5mm 4P	2	Elfa Distralec	12,00 kr
Stiftlist Raster 5mm 4P	2	Elfa Distralec	7,00 kr
Crimp kontakthus Poler 5	3	Elfa Distralec	23,00 kr
Crimphylsa 3A Hona	20	Elfa Distralec	35,00 kr
Stiftlist 1x8P	2	Elfa Distralec	6,00 kr
Crimphölje	5	Elfa Distralec	8,00 kr
Crimphölje	5	Elfa Distralec	12,00 kr
Crimphölje	5	Elfa Distralec	14,00 kr
Crimp-kontakt Hona	35	Elfa Distralec	57,00 kr
littlefuse	5	Elfa Distralec	35,00 kr
Tvinnat pappersgarn 2kg kon	1	Lankava	300,00 kr
pappersgarn,0.8 Nm,200g	1	Lankava	50,00 kr
Platt pappersband,100g	1	Lankava	45,00 kr
Tunt pappersgarn 1.65 Nm,100g	1	Lankava	50,00 kr
Raffia pappersgarn-Fibra Natura	1	Lankava	35,00 kr
Tunt pappersgarn 1.65 Nm,100g	3	Lankava	150,00 kr
Makergear M2+ spare parts	1	Makergear	21 000,00 kr
Wire harness	3	ultimachine	94,00 kr
Självhäftande värmefolie 3M 8810 80x80mm	1	Electrokit	59,00 kr
Servo - micro	2	Electrokit	238,00 kr
Servonav Futaba standard	2	Electrokit	118,00 kr
		Total	29 436,00 kr

Cost of Postage and administrative fees		
Freight	3d-Prima	100,00 kr
invoice fee	3d-Prima	50,00 kr
Freight	kullager.se	130,00 kr
invoice fee	Creative tools	36,00 kr
Freight	Bondtech	306,00 kr
Freight	Electrokit	99,00 kr
Avhasplingsavgif	Nordbergstekniska	63,00 kr
Avhasplingsavgif	Nordbergstekniska	63,00 kr
Avhasplingsavgif	Nordbergstekniska	63,00 kr
Avhasplingsavgif	Nordbergstekniska	63,00 kr
invoice fee	3d-grottan	30,00 kr
Freight	3d-grottan	118,00 kr
Freight	3d-grottan	118,00 kr
invoice fee	3d-grottan	30,00 kr
Freight	Elfa Distralec	150,00 kr
Freight	Elfa Distralec	150,00 kr
Freight	Elfa Distralec	150,00 kr
Freight	Lankava	200,00 kr
Freight	Lankava	200,00 kr
Freight	Makergear	4 000,00 kr
Freight	Ultimachine	263,00 kr
Freight	Electrokit	99,00 kr
	Total	6 481,00 kr
Sum total of project costs		35 917,00 kr

I Cutting Mechanism

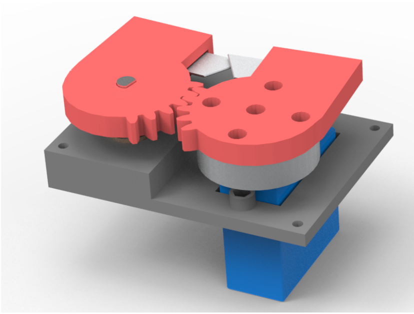

Figure 39: Back view of the mechanism

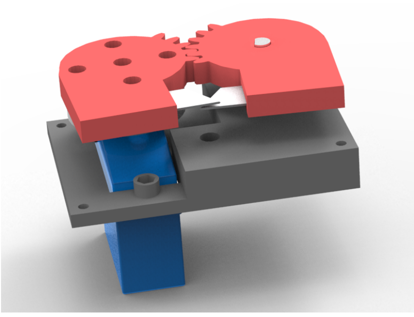

Figure 40: Front view of the mechanism

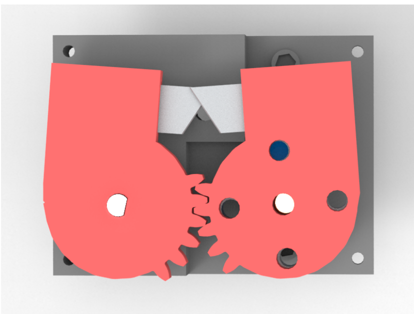

Figure 41: Top view of the mechanism

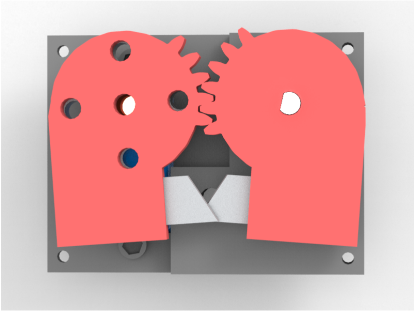

Figure 42: Top view of the mechanism

The blue part is the servo and the read gear-arms are printed in PLA and mounted to the motor with an aluminium nave.

References

[1] T. Terry, T. Caffrey, and R. I. Campbell, *Wohlers report 2016: 3D printing and additive manufacturing state of the industry : annual worldwide progress report*. Wohlers, 2016.

[2] T. Campbell, C. Williams, O. Ivanova, and G. Banning, "Could 3d printing change the world? technologies, potential, and implications of additive manufacturing," *Atlantic Council*, 2011.

[3] K. V. Wong and A. Hernandez, "A review of additive manufacturing," *International Scholarly Research Network*, vol. 10, 2012.

[4] S. B. Allin, "Applied polymer science: 21st century (edited by craver, clara d.; carraher, charles e., jr.," *J C Educ*, vol. 79, p. 942–942, 2002.

[5] E. Teuten, S. Rowland, T. Galloway, and R. Thompson, "Potential for plastics to transport hydrophobic contaminants," *Environ Sci Technol*, vol. 41, pp. 7759–7764, 2007.

[6] C. Rochman, M. Browne, B. Halpern, B. Hentschel, and E. Hoh, "Classify plastic waste as hazardous," *Nature*, vol. 494, pp. 169–171, 2013.

[7] Y. Mato, T. Isobe, H. Takada, H. Kanehiro, and C. Ohtake, "Plastic resin pellets as a transport medium for toxic chemicals in the marine environment," *Environ Sci Technol*, vol. 35, pp. 318–324, 2001.

[8] M. Eriksen, L. C. M. Lebreton, H. S. Carson, M. Thiel, C. J. Moore, J. C. Borerro, F. Galgani, P. G. Ryan, and J. Reisser, "Plastic pollution in the world's oceans: More than 5 trillion plastic pieces weighing over 250,000 tons afloat at sea.," *PLoS ONE*, vol. 9, no. 12, 2014.

[9] A. Amin, S. M. Sauid, and K. Hamid, "Polymer-starch blend biodegradable plastics: An overview," *Advanced Materials Research*, vol. 1113, pp. 93–98, 2015.

[10] N. A. Azahari, N. Othmann, and H. Ismail, "Biodegradation studies of polyvinyl alcohol /corn starch blend films in solid and solution media," *Journal of Physical Science*, vol. 22, no. 2, p. 15–31, 2011.

[11] SEKAB, "Newsletter - december 2015, http://www.sekab.com/media/newsletter/," 2015.

[12] Skogsindustrierna, "Skogsindustrin. en faktasamling. branschstatistik 2014," 2014.

[13] H. Granberg, S. Lindberg, F. Berthold, and M. Lindström, "It's a bird! it's a plane! it's a super multimaterial," in *Proceedings of PaperCon at Georgia World Congress Center*, Innventia, April 2015.

[14] M. K. Zia, M. Zuber, A. Noreen, S. Tabasum, and M. Mujahid, "Recent developments and future prospects on bio-based polyesters derived from renewable resources: A review.," *International Journal of Biological Macromolecules*, vol. 82, pp. 1028–1040, 2015.

[15] J. Lunt, "Large-scale production, properties and commercial applications of polyactic acid polymers," *Polymer Degradation and Stability*, vol. 59, pp. 145–152, 1998.

[16] C. H. Holten, *Lactic Acis Properties and Chemistry of Lactic Acid and Derivatives.* Verlag Chemie, Germany, 1971.

[17] C. Boopathi, S. K. Sundaram, S. Jayabal, and S. Karthikeyan, *Influence of Curing Temperature and Fiber Volume Fraction on the Mechanical Properties of Sisal Fiber Reinforced Polyester Composites*, vol. 3, issue 7. International Journal of Innovative Research in Science, Engineering and Technology, 2014.

[18] S.M.Sapuan, M. Harimi, and M. A. Maleque, *Mechanical Properties of Epoxy/Coconut Shell Filler Particle Composites.* Department of Mechanical and Manufacturing Engineering, Universiti Putra Malaysia and Department of Mechanical and Materials Engineering, Universiti Malaya, 2003.

[19] S. M. Sapuan, A. Leenie, M. Harimi, and Y. K. Beng, *Mechanical Properties of Woven Banana Fibre Reinforced Epoxy Composites.* Department of Mechanical and Manufacturing Engineering, Universiti Putra Malaysia and School of Engineering and Information Technology, Universiti Malaysia Sabah, 2005.

[20] M. R. Sanjay, G. R. Arpitha, L. L. Naik, K. Gopalakrishna, and B. Yogesha, *Applications of Natural Fibers and Its Composites: An Overview*, vol. 7. Natural Resources, 2016.

[21] "Egenskaper hos barrträ, http://www.svensktra.se/om-tra/att-valja-tra/fran-timmer-till-planka/egenskaper-hos-barrtra/," 2016.

[22] R. M. Jones, *Mechanics of Composite Materials.* Taylor & Francis Inc., second ed., 1999.

[23] V. K. Thakur and M. K. Thakur, *Processing and Characterization of Natural Cellulose Fibers/Thermoset Polymer Composites*, vol. 109 http://dx.doi.org/10.1016/j.carbpol.2014.03.039. Carbohydrate Polymers, 2014.

[24] A. C. Long, *Composites forming technologies.* Woodhead Publishing, Cambridge, 2007.

[25] H. Vomhoff, F. Berthold, P. Mäkelä, M. Lindström, K. Wickholm, K. Gamstedt, T. Iversen, T. Lindström, and A. Stenman, "Method for manufacturing a composite material having reduced mechanosorptive creep, the composite material, use of the method and the composite material," no. CA2692780A1, EP2171154A4, US20100193116, WO2009008822A1, 2009.

[26] C. J. Biermann, *Handbook of Pulping and Papermaking.* Academic press limited, 1996.

[27] S. o. M. S. Head and h.-t.-i.-e. Engineering, UNSW Australia, "Extrusion," 2013.

[28] E. Oberg, F. D. Jones, H. L. Horton, and H. H. Ryffel, *Machinery's handbook*, vol. 28th edition. Industrial Press, New York, 2008.

[29] J. Frankland, "The truth about barrel heating, http://www.ptonline.com/columns/the-truth-about-barrel-heating," 2011.

[30] "Colorfabb, http://colorfabb.com/woodfill-fine," 2016.

[31] F. Ning, W. Cong, J. Qiu, J. Wei, and S. Wang, "Additive manufacturing of carbon fiber reinforced thermoplastic composites using fused deposition modeling," *Composites Part B: Engineering*, vol. 80, pp. 369–378, Oct. 2015.

[32] H. L. Tekinalp, V. Kunc, G. M. Velez-Garcia, C. E. Duty, L. J. Love, A. K. Naskar, C. A. Blue, and S. Ozcan, "Highly oriented carbon fiber–polymer composites via additive manufacturing," *Composites Science and Technology*, vol. 105, pp. 144–150, Dec. 2014.

[33] M. Ryosuke, U. Masahito, N. Masaki, J. Tae-Kun, A. Hirosuke, H. Keisuke, N. Taishi, T. Akira, and H. Yoshiyasu, "Three-dimensional printing of continuous-fiber composites by in-nozzle impregnation," *Scientific Reports*, vol. 6, p. 23058, Mar. 2016.

[34] Markforged, "www.markforged.com," 2016.

[35] N. P. Cheremisinoff, *Advanced Polymer Processing Operations*. William Andrew Inc, 1998.

[36] M. Technologies, "How paper-based 3d printing works, http://www.mesa-cad.com/portals/0/mcor/how-paper-based-3d-printing-works.pdf," 2013.

[37] "Makergear m2, http://www.makergear.com/products/m2," 2016.

[38] "Makergear wiki, http://makergear.wikidot.com," 2016.

[39] A. Morar, "Study on modelling and simulation of permanent magnet stepping motor by matlab/simulink," 2014.

[40] "Dmos microstepping driver with translator and overcurrent protection http://www.allegromicro.com/ /media/files/datasheets/a4982-datasheet.ashx," 2014.

[41] Johnnyr, "Rambo, http://reprap.org/wiki/file:rambo1-2-conn-main.jpg," 2014.

[42] "Datasheet, kysan electronics stepper motor," 2012.

[43] "Simulink stepper motor model, https://se.mathworks.com/help/physmod/sps/powersys/ref/steppermo 2017.

[44] "Nordbergs Tekniska AB - fysisk se detail," 2016.

[45] "Kysan elecronics 1040252," 2016.

[46] "Arduino - arduino board nano https://www.arduino.cc/en/main/arduinoboardnano," 2016.

[47] "Pololu - drv8825 stepper motor driver carrier, high current, https://www.pololu.com/product/2133," 2016.

[48] "Drv8825 drv8825 stepper motor controller ic http://www.ti.com/lit/ds/symlink/drv8825.pdf," 2016.

[49] "Diptrace download, http://diptrace.com/download-diptrace/," 2016.

[50] "laurb9/StepperDriver," 2016.

[51] "Pololu - drv8825 stepper motor driver carrier, high current," 2016.